WOOD PHYSICAL PROPERTY MEASUREMENTS USING MICROWAVES

by

JIANPING SHEN
B.E., Jilin University of Technology, 1983
M.E., Zhejiang University, 1986

A THESIS SUBMITTED IN PARTIAL FULFILLMENT OF
THE REQUIREMENTS FOR THE DEGREE OF
DOCTOR OF PHILOSOPHY

in

THE FACULTY OF GRADUATE STUDIES
(Department of Mechanical Engineering)

We accept this thesis as conforming
to the required standard

THE UNIVERSITY OF BRITISH COLUMBIA

April 1996

In presenting this thesis in partial fulfilment of the requirements for an advanced degree at the University of British Columbia, I agree that the Library shall make it freely available for reference and study. I further agree that permission for extensive copying of this thesis for scholarly purposes may be granted by the head of my department or by his or her representatives. It is understood that copying or publication of this thesis for financial gain shall not be allowed without my written permission.

Department of MECH. ENG.

The University of British Columbia
Vancouver, Canada

Date 04/24/96

DE-6 (2/88)

ABSTRACT

The work described in this thesis is the first part of a project aimed at developing an advanced lumber strength grading system using microwave measurements. The overall objective is to develop an improved practical system for estimating lumber strength. A microwave instrumentation system is described in this thesis that can measure wood grain angle, specific gravity, and moisture content. These three physical properties directly influence lumber strength.

In the development of the current microwave instrumentation system, an advanced microwave sensor system was designed to measure elliptically polarized microwave fields. A simplified microwave theory is presented to describe the relationship between the measurements from the sensor and wood grain angle, specific gravity, and moisture content. The simplified theory is very successful in explaining the experimental observations, and provides valuable guidance in the determination of grain angle, specific gravity, and moisture content using the microwave measurements from the new sensor system. Starting from the simplified microwave theory, a simple but efficient model is developed for determining the grain angle using the microwave measurements from the newly developed microwave sensor. For data collected from one hundred samples of Douglas-fir and spruce, the model gave a coefficient of determination $r^2 = 95\%$, and a standard error of 1.8 degrees for grain angles up to 30 degrees.

Simple yet efficient models for evaluating specific gravity and moisture content are also developed. For specific gravity, the proposed evaluation model gives a coefficient of determination $r^2 = 88\%$, and a standard error of 0.026. For moisture content, the proposed evaluation model gives a coefficient of determination of 85% and a standard error of 0.7% in *MC*. Detailed study shows that the current microwave instrumentation system and the developed evaluation models are equally effective for measurement environments such as sawmills where temperature changes seasonally over a substantial range.

The current microwave instrumentation system developed during this thesis research can provide accurate grain angle, specific gravity, and moisture content in real-time regardless of environmental temperature, wood species, and wood structural characteristics such as annual ring direction, diving grain, and small thickness variation. Accurate knowledge of grain angle, specific gravity, and moisture content will make it possible to calculate lumber strength using mechanistic procedures. This will make lumber strength evaluation more accurate and reliable.

TABLE OF CONTENTS

LIST OF FIGURES

NOMENCLATURE

a_i = material calibration constants

b_i = material calibration constants

c_i = material calibration constants

c_A = temperature coefficient of amplitude measurement

c_P = temperature coefficient of phase measurement

d = lumber thickness

d_i = material calibration constants

j = $\sqrt{-1}$, complex number

n = material calibration constants

A_{f0} = amplitude measurement from the scattering dipole parallel to the electric field

A_{f-45} = amplitude measurement from the scattering dipole aligned -45° to the electric field

A_{f45} = amplitude measurement from the scattering dipole aligned 45° to the electric field

A_{f90} = amplitude measurement from the scattering dipole perpendicular to the electric field

A_0 = normalized amplitude measurement from the scattering dipole parallel to the electric field

A_{-45} = normalized amplitude measurement from the scattering dipole aligned -45° to the electric field

A_{45} = normalized amplitude measurement from the scattering dipole aligned 45° to the electric field

A_{90} = normalized amplitude measurement from the scattering dipole perpendicular to the electric field

A_* = $(A_{-45} + A_{45})/2$

$\overline{A}$ = $(A_0 + A_*)/2$

E_I = incident electric field

E_T = transmitted electric field

E_{IP} = incident electric field along the grain direction

E_{IT} = incident electric field across the grain direction

E_{TP} = transmitted electric field along the grain direction

E_{TT} = transmitted electric field across the grain direction

$\tilde{E}$ = electric field in complex form

MC = dry basis moisture content

P_0 = phase measurement from the scattering dipole parallel to the electric field

P_{-45} = phase measurement from the scattering dipole aligned -45° to the electric field

P_{45} = phase measurement from the scattering dipole aligned 45° to the electric field

P_{90} = normalized amplitude measurement from the scattering dipole perpendicular to the electric field

P_* = $(P_{-45} + P_{45})/2$

$\overline{P}$ = $P_0/\cos\theta$

SG	=	specific gravity
α	=	attenuation constant
α_P	=	attenuation constant along the grain direction
α_T	=	attenuation constant across the grain direction
β	=	phase constant
β_P	=	phase constant along the grain direction
β_T	=	phase constant across the grain direction
ε	=	dielectric constant
ε'	=	real part of the dielectric constant
ε''	=	imaginary part of the dielectric constant
γ	=	propagation constant
θ	=	grain angle
$\tan\delta$	=	$\varepsilon''/\varepsilon'$, loss tangent

ACKNOWLEDGMENT

This thesis is dedicated to my parents, my wife Ming, and my son Nicholas. Their love, caring, and encouragement have made this possible.

I would like to thank my supervisor Dr. Gary Schajer for his support and many helpful thoughts, and for the many hours he's spent with me during the study. I would also like to thank Dr. Robert Parker for his technical guidance, Dr. Ray King and Mr. Jesse Basuel at KDC Corporation for their technical assistance in supplying the microwave equipment. Sincere thanks are also due to my thesis advisory committee members Dr. Stavros Avramidis, Dr. Ricardo Foschi, and Dr. Mark Halpern. The kind support and assistance of Dr. Ian Hartley, Mr. Darrell Wong, Mr. Don Bysouth, and members of the Mechanical Engineering machine shop is also much appreciated.

The research in this thesis is funded by the Natural Sciences and Engineering Research Council of Canada (NSERC).

1.0 INTRODUCTION

1.1 Background

Lumber has long been an important construction material because it is easy to use, readily available, economical, and renewable. But as a natural material, its great diversity in physical and mechanical properties makes it extremely difficult to use efficiently. In engineering design, material strength is certainly a major concern. Effective strength grading enables high-strength lumber to be chosen for critical structural applications, while lower strength material can be set aside for less stringent situations [1, 2, 3]. Thus, lumber resource can be utilized according to its capabilities.

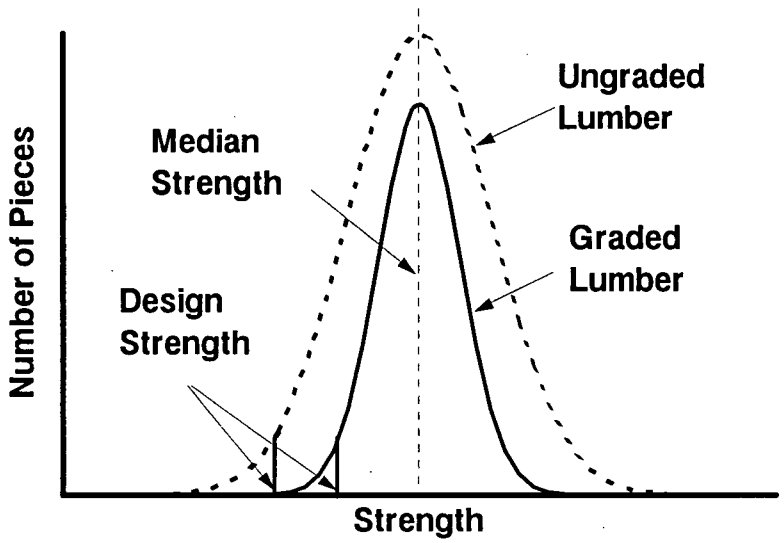

Figure 1-1 Strength Variation within a Batch of Lumber

Figure 1-1 schematically shows how lumber grading increases the design strength of the graded material so that the design strength is closer to the median strength. Lumber strength typically has the bell-shaped distribution shown by the dashed line. Variations in wood properties due to natural growth characteristics causes this curve to be very wide. Structural safety considerations demand that the design strength be set according to the strength of the weakest pieces. That way the majority of the pieces, typically 95%, can be relied upon to support the specified load. However the wide distribution of the strength of ungraded lumber means that the median strength is much greater than the design strength. Thus, the majority of the pieces are seriously under-utilized. Clearly, if it were possible to sort the ungraded lumber into grades with narrower strength distributions, then a much more efficient relationship between design strength and median strength could be obtained. The solid line in Figure 1-1 shows the reduced strength variation that can be achieved by accurate grading. Here the grade has been chosen to have the same median strength as the original ungraded material. In this case, the grading has allowed an increased design strength to be used, even though the median strength of the material is unchanged. This feature greatly improves the efficiency of utilization of lumber by having a much closer relationship between the design strength and the strength of the majority of pieces in that grade.

1.2 Lumber Grading Methods

In industrial practice, lumber is sorted into strength categories (or "grades") using one or more of several available methods. A major objective is to separate the material into grades with the narrow strength distribution indicated by the solid line in Figure 1-1.

The most reliable method for assessing the strength of a piece of lumber is to measure the applied force or moment required to break the piece. Such totally destructive testing is useful for research and for statistical quality control. However, it is clearly not useful for production applications. Non-destructive or minimally destructive strength estimation methods are therefore needed.

Non-destructive strength assessment involves measurement of lumber properties that relate in some way to lumber strength, rather than measuring strength directly. Such strength indicators include visual appearance, grain deviation, specific gravity, and bending stiffness. The quality of grading depends on the number of indicators used, the quality of the indicators and measurements, and the way the strength indicators are used.

1.2.1 Visual Grading

Lumber grading started with the visual grading system about 80 years ago [2]. The visual grading system uses the average strength of small clear wood specimens as a basis and then applies various strength reduction factors to obtain the lumber strength [1]. The strength reduction factors account for the defects in the lumber, including knots, grain deviation, wane, splits, decay, etc. In a mill, an experienced grader inspects each

piece of lumber for visual defects and assigns grades. In this grading system, a lot of visual information is used, but the quality of the information is normally low and subjective. Hence, the effectiveness of visual grading is rather low for strength prediction.

1.2.2 Proof Loading

Besides the lack of consistency of visual grading for strength prediction, the validity of deriving design strength from tests on small clear specimens in the visual grading system has also been in question [33]. The proof load method was introduced to derive lumber mechanical properties from tests conducted directly on full-sized lumber pieces [34-36]. The proof load method involves testing a large sample of lumber from a production population with a predefined load, and then statistically characterizing the design strength of the whole population [34, 35]. During the proof load test, the load has to be held constant over a reasonable time period, hence the proof load method is time-consuming. The proof load is set so that about 10% of the sample is destroyed. This proof load level gives a balance between the value increase from grading and the economic loss induced by the breakage of the material [36]. The proof load method is essentially a destructive method, which incurs economic loss to the mills. Also, proof load testing could cause microscopic damage to the surviving lumber pieces, and reduce their strength [37].

1.2.3 Machine Stress Rating

A second generation method of lumber grading is the machine stress rating (MSR) system, which is based on the correlation between lumber strength and its bending stiffness [1, 2, 3]. The term "MSR" broadly includes all automatic lumber grading systems. In keeping with industrial practice, the term MSR is used here specifically to refer to bending type machines. Typically, the stress rating machines measure the flatwise bending stiffness of lumber over a 1.2-meter span continuously along the lumber length [3]. The minimum and the average stiffness readings are then used to predict strength using pre-calibrated statistical models. Because typical defects in lumber are much smaller than the 1.2-meter bending test span, the effects of local defects in lumber are not well indicated by the measured bending stiffness [10]. Previous researchers [3] reported a moderate coefficient of determination around 50%, which translates into a correlation coefficient of 0.7.

Different wood species have different physical properties, mainly the density and growth characteristics. However, the machine stress rating system does not consider these important material properties directly. This factor results in a difficulty in grading mixed species [3].

The MSR system essentially relies on the modulus of elasticity as the strength predictor. Published research [43, 44] indicates that the modulus of elasticity can only explain about 50% of the strength variation in lumber. This feature limits the grading accuracy of the current MSR system [3, 10, 45] and seriously challenges the possibility of future improvement of such systems.

1.2.4 Vibration Testing

Stemming from the same basis as the MSR system, i.e., the statistical correlation between lumber bending stiffness and strength, the vibration method serves an alternative strength grading procedure. The vibration method determines the modulus of elasticity of a length of lumber by measuring the weight of the piece, and the frequency of transverse vibration. The Model 340 Transverse Vibration E-Computer from Metriguard Inc. is a typical instrument for vibration testing [38]. In this case, the measurement resolution is the lowest possible, the whole length of the lumber piece. Therefore, the effectiveness of the vibration method as a lumber grading tool is only moderate.

1.2.5 Ultrasonic Testing

Another technique using the modulus of elasticity as the strength indicator is the ultrasonic method. The ultrasonic method measures the propagation speed of a longitudinal stress wave traveling from one end of a lumber piece to the other end. The wave speed gives a measure of the elastic modulus of the lumber, which is then used as a statistical indicator of the lumber strength[39-43]. Typically, the measurement is done along the whole length of the lumber. Again, the grading effectiveness in such a system is limited by the quality of the relationship between low-resolution modulus of elasticity measurements and the strength of lumber.

1.2.6 X-Ray Grading

A third generation lumber grading method is based on x-ray densitometry [11]. The X-Ray Grading (XRG) system scans lumber in 1" spatial resolution , which is a substantial improvement over the 48" resolution in the MSR systems. Instead of measuring bending stiffness, the XRG method uses longitudinal density profile and knot information as strength indicators. The XRG system performs better than the MSR system mainly because the measurement resolution is much finer, and more closely corresponds to the size of strength controlling features such as knots. Typical coefficients of determination are around 65-70%, corresponding to correlation coefficients in the range 0.8-0.85. These results are significantly superior to those of the MSR system.

1.2.7 Summary of Strength Grading Methods

The evolution of lumber strength grading from visual system to the various types of mechanical systems sees the automation of grading, and improved measurement quality of the strength indicators. But the indicators are generally mechanical quantities, instead of direct wood properties. Representing more recent technology, the XRG scanning system uses direct material properties as strength indicator. Also, it continues to improve measurement quality of indicators, including higher accuracy and spatial resolution. The XRG scanning system collects over hundred times more information than the current MSR machines do. Figure 1-2 summarizes the key features of the existing lumber grading methods and gives some perspective on possible future grading systems. For improved grading efficiency, a future system should use more fundamental lumber

strength controlling characteristics as strength indicators and be able to measure these characteristics in a spatial resolution comparable to typical lumber defect sizes.

	INDICATORS	RELEVANCE OF INDICATOR TO MATERIAL	QUALITY OF MEASUREMENT	EFFECTIVE-NESS OF GRADING
VISUAL GRADING	Visual Defects	Moderate	Moderate	Low
PROOF LOADING	Proof Load	Strong	Moderate	Moderate
MACHINE STRESS RATING	Bending Stiffness	Moderate	Good, Low Resolution	Moderate
VIBRATION TESTING	Modulus of Elasticity	Moderate	Good, Very Low Resolution	Moderate
ULTRASONIC TESTING	Modulus of Elasticity	Moderate	Moderate to Good	Moderate
X-RAY SCANNING	Density Profile and Knots	Strong	Good, High Resolution	Good
FUTURE GRADING SYSTEM	Grain Deviation, Density, Moisture Content	Strong	Good, High Resolution	Expected to be better

Figure 1-2 Evolution of Lumber Grading System

The next section describes some physical characteristics of wood that control lumber strength. These characteristic will be examined to see how they may be measured and used to provide a superior estimate of lumber strength.

1.3 Non-destructive Measurement of Wood Properties

Many factors influence lumber strength. The main issue in lumber grading is to measure nondestructively the fundamental physical characteristics that control wood strength. These fundamental physical measurements allow a mechanistic evaluation of wood strength to be made, rather than the more common statistical correlation. Since mechanistic calculations model actual wood physical behavior, they are expected to handle effectively the large variations that naturally occur in commercial lumber. In contrast, statistically based methods deteriorate in effectiveness when the graded material deviates in any significant way from the lumber sample used for the original strength correlation testing.

1.3.1 Strength Controlling Features

It is well known, grain deviation, knots and their locations, specific gravity (*SG*), and moisture content (*MC*) are among the most significant strength controlling features in lumber. The first two factors describe the effects of structural defects in lumber, and the last two factors identify the material properties. Among these factors, grain deviation is the most dominant usually. The effect of grain deviation in wood strength can be approximated using a Hankinson-type formula [1]:

$$N = \frac{PQ}{P\sin^n\theta + Q\cos^n\theta} \tag{1-1}$$

where N represents the strength property at an angle θ from the fiber direction, Q is the strength perpendicular to the grain, P is the strength parallel to the grain, and n is an empirically determined constant. n is between 1.5 to 2 for both tensile and bending strength, Q/P is 0.04 to 0.07 for tensile strength and 0.04 to 0.1 for bending strength [1]. Figure 1-3 illustrates equation (1-1) for some typical values of Q, P, and n. It shows that a 5° grain deviation can reduce lumber strength as much as 20%.

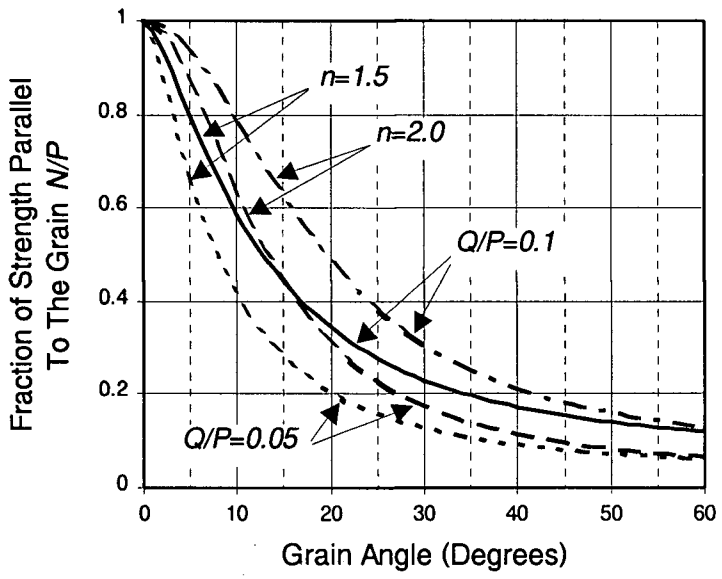

Figure 1-3 Effect of Grain Angle on Strength

Though not as dominant as grain direction, specific gravity and moisture content also have significant effects on lumber strength [1, 4, 5]. It is a common knowledge that

wood of most species floats in water, but the actual wood substance for all species is heavier than water. In fact, wood as a material consists of wood substance, voids, and substrates. Only wood substance is responsible for carrying load. The specific gravity of wood indicates the amount of wood substance per volume. Therefore, the larger the specific gravity the stronger the wood is at the same moisture content.

Dry wood is stronger than wet wood. In general, clear wood strength increases with decreasing moisture content. The shrinkage and swelling of wood accompanying moisture change makes strength change in actual lumber member rather complicated, especially in bending where its load carrying capacity is heavily dependent on its dimension.

At present, lumber strength grading is done without considering the strength controlling factors individually [2, 3]. Cramer and coworkers [6, 7] have shown that lumber tensile strength prediction can be significantly improved with the aid of local grain angle measurements. Using different approaches, Bechtel and Allen [8, 9] have also demonstrated much improved lumber tensile strength evaluation using grain angle information. Improved strength estimates can be achieved if localized lumber physical properties such as grain direction, specific gravity, and moisture content, are taken into account. The ability to measure grain direction, specific gravity, and moisture content will play an important role in the development of next generation lumber strength grading systems. Measuring all these three properties simultaneously is a difficult issue. For lumber grading purposes, the measurements have to be taken in real-time at mill production rates. This poses significant technical challenges.

Specific gravity and moisture content of wood can be measured by drying and weighing, which is normally a destructive process. Available modern equipment using high-energy radiation technology (typically Gamma rays or X-Rays) [11] and video scanning [12] only give the density of wood, not the individual values of specific gravity and moisture content.

Wood grain angle can be measured manually on a clear surface. This method is extremely time-consuming and therefore is impractical for lumber grading on a production line. Grain angle can also be estimated visually, as in visual grading practice [1], but the large error associated with visual estimation often results in inaccurate lumber grading.

1.3.2 Microwave Measurements

Microwave transmission or reflection measurements provide an interesting new approach to measuring wood physical properties. For materials which are semi-transparent to microwaves, their dielectric properties are often very good indicators of their physical properties. The dielectric properties of wood contain information on grain direction, specific gravity, and moisture content [13, 14, 15]. This feature has initiated a great interest in the development of dielectric sensor based measurement instrumentation systems [16, 17, 18]. The nondestructive nature of microwave testing has made it an important measurement means in various application fields [19-24].

Microwave measurement of density has been extensively studied and widely used. Research and application on isotropic materials, such as grain, coal, and particle-board

(in-plane isotropic), has been very successful [19-24]. When microwaves transmit through a material, they experience power loss and speed reduction. Both these features can be readily measured using various microwave detection systems [25]. Proper modeling of the attenuation and phase change can not only provide the specific gravity, but also the moisture content. This capability makes microwave measurements potentially superior to X-Ray measurements because the latter normally only give the total density (wood+moisture). The radiation safety concern also puts the X-Ray systems at a disadvantage. Since many material factors in solid wood are coupled with grain angle, automatic detection of specific gravity, and moisture content is much more complicated in lumber, especially when localized measurement is pursued. The specific gravity and moisture content have to be measured together along with the grain angle information.

The dielectric anisotropy associated with wood fiber direction provides an excellent means for grain angle detection. The dielectric constant of wood is largest along the grain, and smallest across the grain [13-15]. A well-established technology for measuring grain angle based on wood dielectric properties is the "Slope-of-Grain Indicator" [26, 27]. A capacitance sensor is mounted close to the wood surface. As the sensor is rotated at the measurement location, the capacitance measured from the sensor is read, and grain angle is characterized accordingly. The required mechanical rotation of the capacitance sensor slows the measurement process significantly. Furthermore, the capacitance sensor can only respond to the material near the lumber surface; it does not probe into the bulk of the material.

The dielectric anisotropy of wood causes a linearly polarized electromagnetic field to be depolarized upon transmission through the material [28]. The degree of depolarization is a direct measure of the grain deviation. By measuring microwave depolarization, the wood grain deviation can be quantified.

One way of measuring the field depolarization is to rotate a scattering dipole in the field [28-30]. Grain angle can then be extracted from the depolarization information. However, the dependence of depolarization on moisture and density makes grain angle prediction rather complicated. The rotation mechanism of the sensor design also complicates and degrades the measurement.

In summary, present density and moisture measurement systems are not adequate for making localized measurements in solid wood because of the complication from grain deviation. New instrumentation must be developed. Considering the coupling between the grain angle, specific gravity, and moisture content, the new instrumentation system has to handle all these three wood properties simultaneously.

The instrumentation system developed for the research described in this thesis employs a stationary design. This feature not only means much higher measurement speed but also greater mechanical ruggedness and lower maintenance cost. The prototype measurement system used in this study can take measurements at a speed up to 40KHz. This speed would vary greatly according to the measurement electronics and computer hardware available. The system measures transmitted microwaves to give an integrated average through the board thickness. This feature is desirable for two-dimensional strength modeling because grain angle measured from one face of the lumber may not

represent the other face. The high microwave frequency and small sensor design in the instrumentation give a comparatively fine spatial measurement resolution of about 2 cm. The same instrumentation system can also provide specific gravity and moisture content.

1.4 Objectives and Organization

A review of the different lumber grading systems available reveals the need for a new generation of lumber strength grading system. This system requires the direct involvement of localized lumber strength controlling factors, mainly the grain angle, specific gravity, and moisture content. The objective of this thesis is to develop a microwave system for measuring grain angle, specific gravity, and moisture content simultaneously. This thesis covers the instrumentation and measurement part of the on-going project of developing a new lumber strength grading system based on microwave technology.

As a foundation, Chapter 2 describes the characteristics of microwave transmission through wood. Then, Chapter 3 gives the layout of the microwave instrumentation system and the details of the design of a new microwave probe that is able to characterize elliptically polarized microwave fields. The new probe is capable of giving wood grain direction, specific gravity, and moisture content simultaneously without mechanical rotation. Chapter 3 further provides the theoretical formulation of the microwave instrumentation system with the new probe for wood property measurement.

Chapter 4 focuses on the experimental measurements. It describes the experimental procedures and the effects from various wood growth characteristics, such as species, ring direction, diving grain, and thickness variation.

Chapter 5 and 6 consider practical procedures for evaluating grain angle, specific gravity, and moisture content from the microwave measurements described in Chapter 4.

Chapter 7 shows the effects of temperature on microwave measurements and the evaluation of wood properties.

Finally, Chapter 8 summarizes the main results and conclusions from the research work described in this thesis, and gives some suggestions for future applications.

2.0 MICROWAVE PROPAGATION THROUGH WOOD

This chapter summarizes a basic theory needed for using microwave measurements to determine wood physical properties. The measurement procedure involves propagating microwave radiation through wood and measuring the transmitted microwave field. Various physical properties of wood can be inferred from the measured differences between the incident and transmitted microwave fields.

When microwave radiation propagates through wood, it experiences power loss (attenuation), speed reduction (phase change), and also depolarization. Microwave propagation through a dielectric material such as wood is characterized by the material dielectric properties. In the simple case of an isotropic material, the dielectric property is expressed by a scalar constant. In an orthotropic material such as wood, however, microwave propagation becomes much more complicated, and a tensor quantity is required to describe the dielectric properties. This chapter discusses the propagation of microwave radiation through wood, and shows how the resulting changes in the transmitted microwave radiation depend on the wood dielectric and physical properties. For simplicity, the more basic case of microwave transmission through an electrically isotropic material is considered first. Then, the isotropic results are generalized to describe transmission through an orthotropic material such as wood.

2.1 Microwave Transmission through an Isotropic Material

Figure 2-1 shows the simple case of microwave radiation propagating through a uniform slab of isotropic material. The electric field of the incident microwave is $\boldsymbol{E}_I$[†].

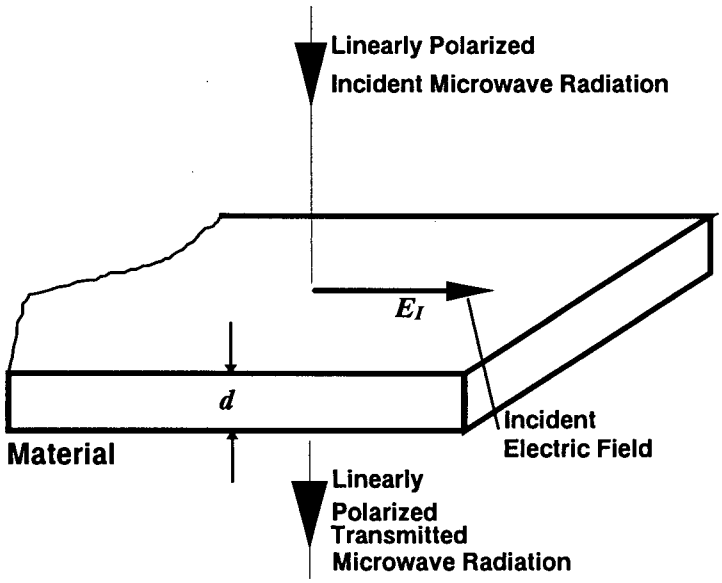

Figure 2-1 Microwave Field Transmission through Isotropic Material

After propagation through the material, the electric field of the transmitted microwave is $\boldsymbol{E}_T$. Reflections at the incident and transmission surface are assumed to be negligible. The relationship between the incident and transmitted electric fields depends on the material properties and thickness of the slab, as follows,

---

† Bold face font indicates vector quantities. Regular font indicates the corresponding magnitudes. For example, E_I is the magnitude of vector $\boldsymbol{E}_I$.

$$E_T = E_I e^{-\gamma d} \tag{2-1}$$

where γ is the propagation constant and d is the slab thickness. The propagation constant γ is a complex quantity,

$$\gamma = \alpha + j\beta \tag{2-2}$$

where α and β are the attenuation and phase constants, respectively, and $j = \sqrt{-1}$. The propagation constant γ can also be written as

$$\gamma = j\beta_0\sqrt{\varepsilon} \tag{2-3}$$

where $\beta_0 = 2\pi/\lambda_0$ is the phase constant in air, λ_0 is the wavelength in air, and ε is the complex dielectric constant,

$$\varepsilon = \varepsilon' + j\varepsilon'' \tag{2-4}$$

The imaginary part ε'' is responsible for the power loss, and is often described by the loss tangent,

$$\tan\delta = \varepsilon''/\varepsilon' \tag{2-5}$$

Propagation of microwave through an isotropic material involves no change in polarization. Thus, if the incident microwave fields are linearly polarized, the transmitted fields will also be linearly polarized in the same direction.

By expressing ε'' in terms of the loss tangent and using binomial expansion, the propagation constant γ can be rewritten as

$$\gamma = j\beta_0 \left[\varepsilon'(1 + j\tan\delta)\right]^{1/2}$$
$$= j\beta_0\sqrt{\varepsilon'}\left(1 + j\frac{\tan\delta}{2} + \frac{\tan^2\delta}{8} + \cdots\right) \tag{2-6}$$

For $\tan\delta << 1$, equations (2-2) and (2-6) give

$$\alpha \approx \frac{\beta_0\sqrt{\varepsilon'}\tan\delta}{2} \tag{2-7}$$

and

$$\beta \approx \beta_0\sqrt{\varepsilon'}\left(1 + \frac{\tan^2\delta}{8}\right) \tag{2-8}$$

In the case of wood, equations (2-7) and (2-8) can be used to qualitatively relate the microwave change upon transmission through wood to the moisture content and specific gravity.

2.2 Effects of Wood Specific Gravity and Moisture Content on Microwave Transmission

To show how wood specific gravity and moisture content affect the change of microwave field after transmitting through wood, it is convenient temporarily to ignore the grain structure of wood and assume that wood is electrically isotropic.

The dielectric properties of wood have been extensively studied motivated by wood drying and wood property measurement using microwaves [13-15, 28, 46]. James and Hamill [15] and Yen [28] have collected extensive data for $\tan\delta$ and ε' for wood. Typically $\tan\delta << 1$ for wood with low moisture content (<30% dry basis). Also, the dielectric constant of wood increases with the moisture content and specific gravity, but

the effect of moisture content is the major factor because the dielectric constant of water is much larger than the dielectric constant of wood substance. James and Hamill [15] show that, at low moisture (below saturation point), ε' is mainly a function of wood density and does not significantly vary with moisture content. However, ε'' and the loss tangent increase rapidly with moisture content. Therefore, from equations (2-7) and (2-8), the microwave power loss (attenuation αd) mainly depends on moisture content, and the phase change (βd) mainly depends on specific gravity. It follows that the moisture content and specific gravity of wood can be quantified by measuring the attenuation and phase change of the electric field of the microwave transmitted through the wood.

2.3 Microwave Transmission through Wood

The distinctive grain structure of wood causes the material to have highly orthotropic properties, both mechanically and electrically. Therefore, microwave propagation in wood is much more complicated than the isotropic case considered in the last two sections.

The dielectric constant and loss tangent of wood are the largest along the grain direction and smallest across the grain [13-15, 28]. In Figure 2-2, which shows wood without diving grain, the orthotropy is two-dimensional. A complete description of microwave transmission in this case requires the 2×2 dielectric tensor

$$\varepsilon = \begin{bmatrix} \varepsilon_P & \varepsilon_{PT} \\ \varepsilon_{TP} & \varepsilon_T \end{bmatrix} \tag{2-9}$$

where all the elements are complex quantities as expressed by equation (2-4). The subscript P stands for parallel, and the subscript T stands for Transverse. The diagonal

terms correspond to the dielectric constants parallel and transverse to the grain direction. The off-diagonal element ε_{PT} is the dielectric constant in the grain direction created by an electric field transverse to the grain direction, and ε_{TP} is the dielectric constant across the grain acquired from an electric field along the grain. Fortunately, the off-diagonal terms are typically only a few percent of the diagonal terms for low moisture content [28]. Thus, the off-diagonal terms will be neglected for simplicity in the following discussions.

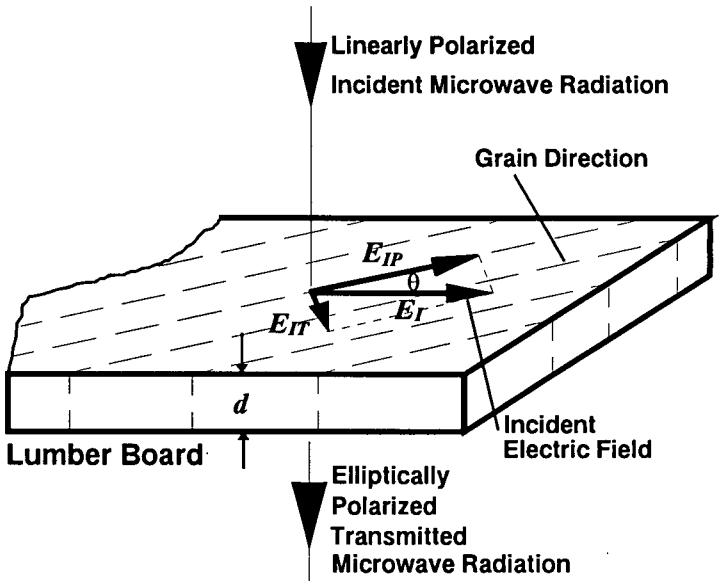

Figure 2-2 Microwave Field Transmission through Wood

As shown in Figure 2-2, the incident electric field $\boldsymbol{E}_I$ can be broken into two components, along the grain $\boldsymbol{E}_{IP}$, and across the grain $\boldsymbol{E}_{IT}$,

$$E_{IP} = E_I \cos\theta \quad \text{and} \quad E_{IT} = E_I \sin\theta \tag{2-10}$$

where θ is the grain angle measured from the incident electric field.

When reflection is negligible, as in the case of low moisture content, the transmitted electric field along the grain and across the grain is described by relationships analogous to equations (2-1) and (2-2),

$$E_{TP} = E_{IP} e^{-(\alpha_P + j\beta_P)d} \tag{2-11}$$

$$E_{TT} = E_{IT} e^{-(\alpha_T + j\beta_T)d} \tag{2-12}$$

where α_P, β_P and α_T, β_T are the attenuation and phase constants in the longitudinal and transverse directions, respectively.

For convenience, the instantaneous electric fields can be mathematically expressed in complex form as,

$$\tilde{E}_I = E_I e^{j(\omega t + \phi)} \tag{2-13}$$

where ω is the microwave frequency, ϕ is the phase angle. Using this notation, the electric field intensities along and across the grain are

$$\begin{aligned} \tilde{E}_{TP} &= E_I e^{j(\omega t+\phi)} \cos\theta \, e^{-(\alpha_P + j\beta_P)d} \\ &= E_I \cos\theta \, e^{-\alpha_P d + j(\omega t + \phi - \beta_P d)} \end{aligned} \tag{2-14}$$

and

$$\begin{aligned} \tilde{E}_{TT} &= E_I e^{j(\omega t+\phi)} \sin\theta \, e^{-(\alpha_T + j\beta_T)d} \\ &= E_I \sin\theta \, e^{-\alpha_T d + j(\omega t + \phi - \beta_T d)} \end{aligned} \tag{2-15}$$

The real parts of equations (2-14) and (2-15) describe the transmitted electric fields. Along the grain, the result is

$$E_{TP} = E_I \cos\theta \, e^{-\alpha_P d} \cos(\omega t + \phi - \beta_P d) \tag{2-16}$$

and across the grain

$$E_{TT} = E_I \sin\theta \, e^{-\alpha_T d} \cos(\omega t + \phi - \beta_T d) \tag{2-17}$$

By eliminating time t in equations (2-16) and (2-17), we obtain

$$\frac{E_{TP}^2}{|E_{TP}|^2} - 2\frac{E_{TP}E_{TT}\cos(\beta_P d - \beta_T d)}{|E_{TP}|\cdot|E_{TT}|} + \frac{E_{TT}^2}{|E_{TT}|^2} = \sin^2(\beta_P d - \beta_T d) \tag{2-18}$$

where $|E_{TP}| = E_I \cos\theta e^{-\alpha_P d}$ and $|E_{TT}| = E_I \sin\theta e^{-\alpha_T d}$ are the amplitudes of the transmitted fields $\boldsymbol{E}_{TP}$ and $\boldsymbol{E}_{TT}$, respectively. Equation (2-18) is the mathematical representation of an ellipse in the P-T plane. Figure 2-3 schematically represents equation (2-18), where the horizontal axis is the longitudinal direction of the lumber. The ellipse is simply the trace of the electric field vector over one cycle. It should be noted that the inclination angle of the ellipse Φ does not normally coincide with the grain angle.

Since both α_P and β_P in equations 2-11 and 2-12 are larger than the corresponding α_T and β_T, the incident field component E_{IP} experiences much larger attenuation and phase change than E_{IT} does. Therefore the transmitted fields, along grain E_{TP} and across grain E_{TT}, are unequally attenuated and suffer unequal phase delays. They therefore emerge with elliptical polarization, which is demonstrated using equations (2-16) and (2-17). When θ is zero or 90 degrees, either E_{TT} or E_{TP} becomes zero according to equations (2-16) and (2-17), i.e., the transmitted field is linearly polarized. Therefore, depolarization from a linearly polarized incident microwave field is avoided only if the incident electric field is exactly aligned along one of the two electrical

symmetry axes of the material, i.e., either parallel or perpendicular to the wood grain direction.

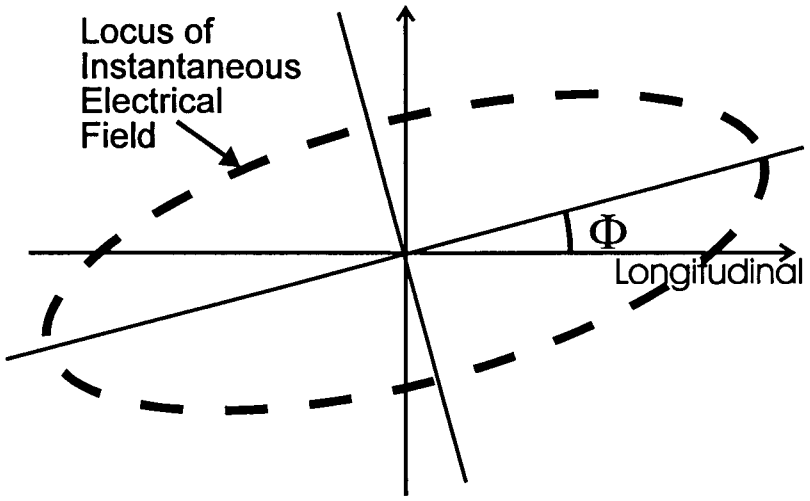

Figure 2-3 Elliptical Polarization

2.4 Chapter Summary and Conclusions

Section 2.1 presented the basic theory of microwave transmission through an isotropic material. Section 2.2 extends the simple isotropic case to relate the transmitted microwave field to the specific gravity and moisture content of wood based on previous findings of the dielectric properties of wood [13-15, 28]. In summary, both the attenuation and phase change of the microwave signal propagating through wood are dependent on the moisture content. By measuring the attenuation and phase change, the moisture content and specific gravity can be determined.

Section 2.3 presented a simplified theory of microwave transmission through wood. The theory shows that the depolarization of a linearly polarized incident microwave field by transmitting through a slab of wood depends on grain angle. Therefore, the wood grain angle can be quantified by measuring the depolarization.

The theory presented in this chapter suggests that it is feasible to measure wood grain direction, specific gravity, and moisture content using microwaves. A complicating factor is that the attenuation and phase change are also functions of the grain direction because of the orthotropic wood dielectric properties. The difference between the dielectric constants along and across the grain is dependent on the specific gravity and moisture content[15]. Hence, the depolarization of microwaves transmitting through wood undesirably contains the influence of specific gravity and moisture content besides grain direction.

Basically, the microwave measurements are dependent on wood grain angle, specific gravity, and moisture content simultaneously. This feature complicates the procedure of determining the grain angle, specific gravity, and moisture content from the microwave measurements though these wood properties themselves are independent. The problem can be solved using a sophisticated instrumentation system along with proper mathematical modeling, which will be shown in the later chapters.

3.0 INSTRUMENTATION SYSTEM

3.1 The Microwave System

This section briefly describes the research prototype microwave measurement system used in this thesis for the measurements of wood properties.

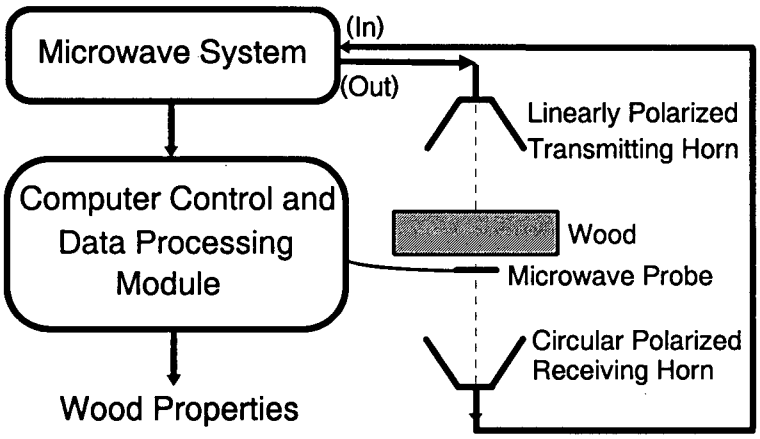

Figure 3-1 Schematic of the Wood Property Measurement System

Figure 3-1 shows a schematic of the prototype system. The microwave system employed in this project uses the homodyne design. Details of the practical implementation can be found in a number of articles by King [25, 30]. The microwave homodyne system uses a coherent detection process to give independent amplitude and

phase information simultaneously. The microwave system in Figure 3-1 consists of a microwave generator, amplitude and phase detectors, as well as various interfaces for computerized control and data acquisition.

The prototype microwave system uses two horn antennae. One of the two is linearly polarized and operates as a microwave transmitter and the other is circularly polarized and functions as a microwave receiver. Linearly polarized microwaves at 10 GHz are transmitted by the transmitting horn antenna and propagate through the wood sample. The microwave probe underneath the wood sample consists of scattering dipoles electrically modulated at 455 kHz. These scattering dipoles have a compact design with a length of about 2 cm for localized measurements. They are described in more detail in the next section. Modulated scattered signals from the probe are received by the circularly polarized receiving horn antenna and then sent to the microwave system for detection. The detected amplitude and phase values are received by the computer and used for predicting wood properties, i.e., the specific gravity, moisture content, and grain angle. The modulation frequency of 455 kHz was chosen mainly because electronic components operating at this frequency are readily available.

3.2 Theory and Design of the New Microwave Probe

After transmission through wood, linearly polarized microwave radiation becomes elliptically polarized. The ability to characterize the transmitted elliptically polarized microwave field is critical in measuring wood properties.

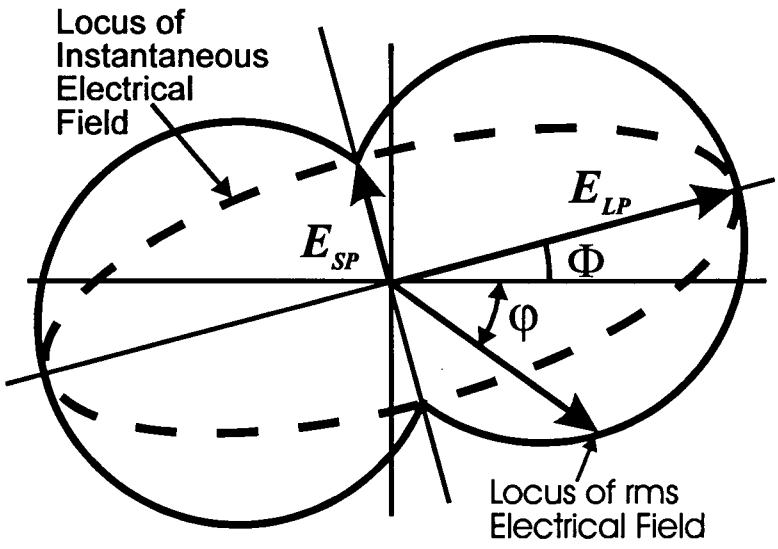

Figure 3-2 Locus of the Instantaneous Electrical Field and $k|E \bullet u|$ Measured from a Dipole

The locus of the instantaneous electrical field of elliptically polarized microwave radiation is an ellipse, with principal radii E_{LP} and E_{SP}. Figure 3-2 shows this ellipse as a dashed line. However, as discussed by King [29], the rms field measured by an

electrically modulated scattering dipole in an elliptically polarized field is not elliptical. The amplitude of the scattered modulated field component can be written as $k|\boldsymbol{E} \bullet \boldsymbol{u}|$, where $\boldsymbol{E}$ is the electric field vector at the dipole, $\boldsymbol{u}$ is the unit vector along the scattering dipole, and k is a constant depending on the dipole geometry [29]. If a scattering dipole is rotated in the polarization plane, the rms of $|\boldsymbol{E} \bullet \boldsymbol{u}|$ sweeps out a pattern consisting of two equal intersecting circles enclosing the instantaneous field ellipse. Figure 3-2 shows these curves as solid lines. For brevity, the double circular pattern is called here a "binocular" curve. Since the instantaneous ellipse and the binocular curve have the same principal radii, the instantaneous field can be measured indirectly by characterizing the circles in Figure 3-2.

One way to characterize the circles in Figure 3-2 is to take measurements while mechanically spinning a dipole in the plane of polarization [30]. This procedure is undesirable because of the mechanical limitations of this method. Also, much of the measured data are redundant because only three independent points are needed to locate a circle in a plane. Thus, a probe that has the capability to measure the rms field in at least three different directions is capable of characterizing the electrical field. Based on the above arguments, a new design of microwave probe in Figure 3-3 has been developed.

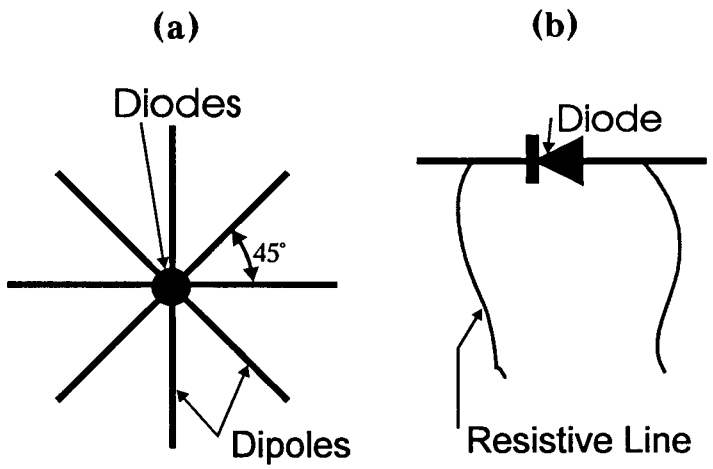

Figure 3-3 Schematic of the New Microwave Probe
(a) assembly of four dipoles
(b) an individual dipole

The new probe consists of four dipoles inclined at 45 degrees to each other. This design contains one more than the minimum number of dipoles because this arrangement was found to improve the computation accuracy. Each dipole of the probe has a pin diode in the middle providing a path for modulation. The modulation signal is carried by highly resistive lines connecting the dipoles to the modulation source. The choice of the resistive lines is made to minimize disturbance to the microwave field.

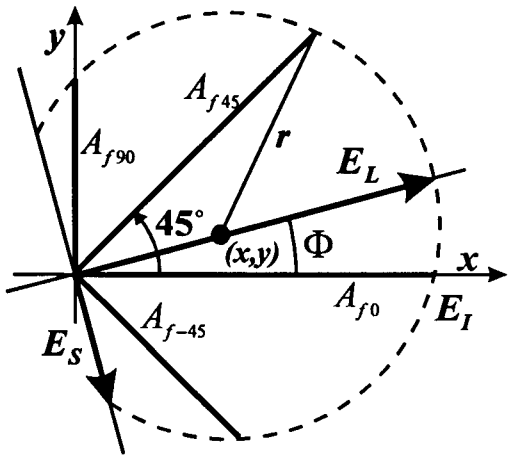

Figure 3-4 Geometric Representation of Measurements from the Probe's Four Dipoles and the Field Vectors

For convenient reference, the four dipoles in the probe are denoted subscripts 0, 45, -45, and 90 according to their relative orientation to the incident electrical field vector E_I. Their measured amplitudes are denoted A_{f0}, A_{f45}, A_{f-45}, and A_{f90}, respectively. The ratio of the field along the major axis E_{LP} to the field along the minor axis E_{SP}, written as E_{LP}/E_{SP}, and the inclination angle Φ can be determined from any three measurements. In Figure 3-4, let (x,y) be the center of the circle and r the radius. From analytic geometry using measurements A_{f0}, A_{f45}, and A_{f90}, the expressions for E_{LP}/E_{SP} and Φ can be written as:

$$x = \frac{\sqrt{2}A_{f90}\left(A_{f0}^{\,2} - A_{f45}^{\,2}\right) + A_{f45}\left(A_{f90}^{\,2} - A_{f0}^{\,2}\right)}{2\sqrt{2}A_{f0}A_{f90} - 2A_{f45}\left(A_{f0} + A_{f90}\right)} \qquad (3\text{-}1)$$

$$y = \frac{2A_{f0}\left(A_{f90}{}^2 - A_{f45}{}^2\right) + \sqrt{2}A_{f45}\left(A_{f0}{}^2 - A_{f90}{}^2\right)}{4A_{f0}A_{f90} - 2\sqrt{2}A_{f45}\left(A_{f0} + A_{f90}\right)} \tag{3-2}$$

$$r = \sqrt{\left(x - A_{f0}\right)^2 + y^2} = \sqrt{\left(x - A_{f45}/\sqrt{2}\right)^2 + \left(y - A_{f45}/\sqrt{2}\right)^2} = \sqrt{x^2 + \left(y - A_{f90}\right)^2} \tag{3-3}$$

$$\Phi = \text{atan}\frac{y}{x} \tag{3-4}$$

$$\left|\frac{E_{LP}}{E_{SP}}\right| = \frac{r + \sqrt{x^2 + y^2}}{\sqrt{r^2 - x^2 - y^2}}. \tag{3-5}$$

The direction of A_{f90} depends on the sign of the inclination angle Φ (positive for counterclockwise). A_{f90} is 90 degrees from A_{f0} when Φ is positive, and is minus 90 degrees from A_0 when Φ is negative (please refer to Figure 3-4).

In practice, the angles between the dipoles may not be perfectly 45 degrees due to fabrication error and small influence of the resistive lines. To eliminate this error in calculation, the dipole directions can be calibrated for each probe. A set of equations for arbitrary dipole directions have also been derived. If the directions of three dipoles are at φ_1, φ_2, and φ_3, and their readings are A_1, A_2, and A_3, respectively, then equations (3-3), (3-4) and (3-5) are replaced by:

$$x = \frac{A_1{}^2\left(S_3 - S_2\right) + A_2^2\left(S_1 - S_3\right) + A_3^2\left(S_2 - S_1\right)}{2\left[C_1\left(S_3 - S_2\right) + C_2\left(S_1 - S_2\right) + C_3\left(S_2 - S_1\right)\right.} \tag{3-6}$$

$$y = \frac{A_1{}^2\left(C_2 - C_3\right) + A_2^2\left(C_3 - C_1\right) + A_3^2\left(C_1 - C_2\right)}{2\left[C_1\left(S_3 - S_2\right) + C_2\left(S_1 - S_2\right) + C_3\left(S_2 - S_1\right)\right]} \tag{3-7}$$

$$r = \sqrt{(x - C_1)^2 + (y - S_1)^2} = \sqrt{(x - C_2)^2 + (y - S_2)^2} = \sqrt{(x - C_3)^2 + (y - S_3)^2} \qquad (3\text{-}8)$$

where

$$\begin{aligned} C_1 &= A_1 \cos\varphi_1, \quad C_2 = A_2 \cos\varphi_2, \quad C_3 = A_3 \cos\varphi_3, \\ S_1 &= A_1 \sin\varphi_1, \quad S_2 = A_2 \sin\varphi_2, \quad S_3 = A_3 \sin\varphi_3. \end{aligned} \qquad (3\text{-}9)$$

These equations are easily processed by a computer.

The performance of the new probe when measuring elliptically polarized microwave fields is confirmed in a previous publication [32]. The measurement results from the new probe match very well with the results from the spinning dipole method, though the new probe method only uses about one-twentieth of the information used in the spinning dipole method. The stationary design of the new probe eliminates the need for the rotational mechanism found in the spinning dipole method, and thus allows much greater measurement speed and improved ruggedness. Both features are important advantages in high-speed industrial applications in harsh environments such as lumber grading in sawmills.

3.3 Wood Measurements Using the New Microwave Probe - Analytical

In order to make wood property measurement, the probe is placed close to the lower surface of the wood, as shown in Figure 3-1. Figure 3-5 shows the relationships between the grain direction, the dipole orientations, and the electric field, where θ is the

grain angle measured from the incident electric field E_I. The probe and wood sample are in the plane normal to of the field propagation direction. Again, this is much simplified two-dimensional description about field transmission in wood as stated before.

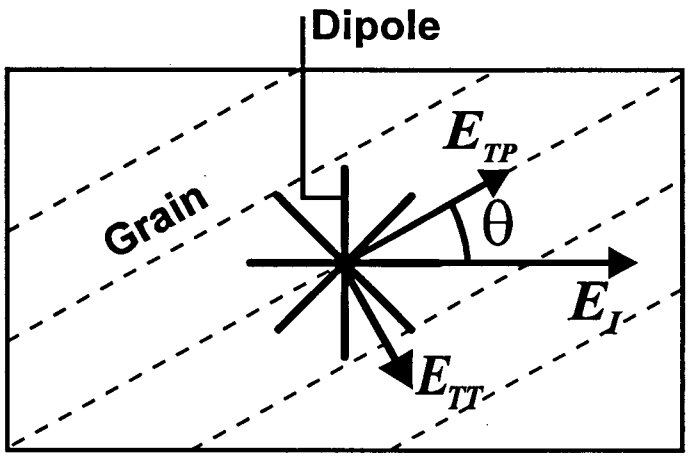

Figure 3-5 Probe Arrangement and Transmitted Fields

The incident electric field components along and across to wood grain direction are presented by equations (2-10). For low moisture content (under fiber saturation point), reflections at the wood and air interfaces may be neglected [28]. Assuming that the propagation constants parallel to grain and transverse to grain are $\gamma_P = \alpha_P + j\beta_P$ and $\gamma_T = \alpha_T + j\beta_T$, respectively, then the transmitted fields are:

$$E_{TP} = E_{IP} e^{-\gamma_P d} = E_0 \cos\theta \, e^{-\alpha_P d + j(\omega t + \beta_P d)} \tag{3-10}$$

and $$E_{TT} = E_{TL} e^{-\gamma_T d} = E_0 \sin\theta \, e^{-\alpha_T d + j(\omega t + \beta_T d)} \tag{3-11}$$

where α's and β's are the attenuation and phase constants, respectively, and d is the lumber thickness. Thus, the transmitted electric field is the sum of $\boldsymbol{E}_{TP}$ and $\boldsymbol{E}_{TT}$. When there is no wood in the field, the electric field along each dipole is:

$$E_0 = E_I = E_0 e^{j\omega t} \tag{3-12}$$

$$E_{45} = E_I \cos 45^\circ = E_0 e^{j\omega t} \cos 45^\circ \tag{3-13}$$

$$E_{-45} = E_I \sin 45^\circ = E_0 e^{j\omega t} \sin 45^\circ \tag{3-14}$$

$$E_{90} = E_I \cos 90^\circ = 0 \tag{3-15}$$

The amplitude readings, A_0^{air}, A_{45}^{air}, A_{-45}^{air}, and A_{90}^{air} from the dipoles are proportional to the mean squares for the right side of equations (3-12) through (3-15), they are:

$$A_0^{air} = E_0^2/2,\ A_{45}^{air} = A_{-45}^{air} = E_0^2/4, \text{ and } A_{90}^{air} = 0 \tag{3-16}$$

When wood is present in the field, the transmitted field along each dipole is:

$$\begin{aligned} E_0 &= E_{TP}\cos\theta + E_{TT}\sin\theta \\ &= E_0 \cos^2\theta \, e^{-\alpha_P d + j(\omega t + \beta_P)d} + E_0 \sin^2\theta \, e^{-\alpha_T d + j(\omega t + \beta_T)d} \end{aligned} \tag{3-17}$$

$$\begin{aligned} E_{45} &= E_{TP}\cos(45^\circ - \theta) - E_{TT}\sin(45^\circ - \theta) \\ &= E_0 \cos(45^\circ - \theta)\cos\theta \, e^{-\alpha_P d + j(\omega t + \beta_P)d} - E_0 \sin(45^\circ - \theta)\sin\theta \, e^{-\alpha_T d + j(\omega t + \beta_T)d} \end{aligned} \tag{3-18}$$

$$\begin{aligned} E_{-45} &= E_{TP}\sin(45^\circ - \theta) + E_{TT}\cos(45^\circ - \theta) \\ &= E_0 \sin(45^\circ - \theta)\cos\theta \, e^{-\alpha_P d + j(\omega t + \beta_P)d} + E_0 \cos(45^\circ - \theta)\sin\theta \, e^{-\alpha_T d + j(\omega t + \beta_T)d} \end{aligned} \tag{3-19}$$

$$
\begin{aligned}
E_{90} &= E_{TP}\sin\theta - E_{TT}\cos\theta \\
&= E_0 \sin\theta\cos\theta\, e^{-\alpha_P d + j(\omega t+\beta_P)d} - E_0\cos\theta\sin\theta\, e^{-\alpha_T d + j(\omega t+\beta_T)d} \\
&= \frac{E_0}{2}\sin 2\theta \left[e^{-\alpha_P d + j(\omega t+\beta_P)d} - e^{-\alpha_T d + j(\omega t+\beta_T)d}\right]
\end{aligned}
\tag{3-20}
$$

After calculating the mean square for equations (3-17) through (3-20), we obtain the dipole amplitude readings with respect to their corresponding values without wood in the field shown in equation (3-16), these normalized amplitudes are:

$$
A_0 = \cos^4\theta\, e^{-2\alpha_P d} + \sin^4\theta\, e^{-2\alpha_T d} + 2\cos^2\theta\sin^2\theta\, e^{-(\alpha_P+\alpha_T)d}\cos(\beta_P d - \beta_T d) \tag{3-21}
$$

$$
\begin{aligned}
A_{45} = {} & 2\cos^2(45^\circ-\theta)\cos^2\theta\, e^{-2\alpha_P d} + 2\sin^2(45^\circ-\theta)\sin^2\theta\, e^{-2\alpha_T d} \\
& -\frac{1}{2}\sin 4\theta\, e^{-(\alpha_P+\alpha_T)d}\cos(\beta_P d - \beta_T d)
\end{aligned}
\tag{3-22}
$$

$$
\begin{aligned}
A_{-45} = {} & 2\sin^2(45^\circ-\theta)\cos^2\theta\, e^{-2\alpha_P d} + 2\cos^2(45^\circ-\theta)\sin^2\theta\, e^{-2\alpha_T d} \\
& +\frac{1}{2}\sin 4\theta\, e^{-(\alpha_P+\alpha_T)d}\cos(\beta_P d - \beta_T d)
\end{aligned}
\tag{3-23}
$$

$$
A_{90} = \frac{A_{90}^{wood}}{A_0^{air}} = \frac{\sin^2 2\theta}{4}\left[e^{-2\alpha_P d} + e^{-2\alpha_T d} - 2e^{-(\alpha_P+\alpha_T)d}\cos(\beta_P d - \beta_T d)\right] \tag{3-24}
$$

From equations (3-21) through (3-24), all the normalized amplitude readings are independent of the incident microwave power. They are all functions of the attenuation constants α_P, α_T and the phase constants β_P, β_T. As the attenuation constants and phase constants are mainly controlled by moisture content and specific gravity, respectively, at low moisture content [15, 28], the normalized amplitudes should reflect

the moisture content and specific gravity of the material. Unfortunately, they are also functions of the grain angle. This coupling between the material properties and the structural factor in solid wood is obviously undesirable as it adds one more variable with nonlinear behavior in modeling the measured data.

By combining the normalized amplitudes, simpler measurement expressions can be obtained. One such expression is the sum of A_{45} and A_{-45}, namely

$$\begin{aligned} A_{+} &= \left(A_{45} + A_{-45}\right)/2 = e^{-2\alpha_P d}\cos^2\theta + e^{-2\alpha_T d}\sin^2\theta \\ &= e^{-2\alpha_P d} + e^{-2\alpha_T d}\left(1 - e^{-2(\alpha_P - \alpha_T)d}\right)\sin^2\theta \end{aligned} \tag{3-25}$$

The advantages of using A_{+} stem from the relative simplicity of equation (3-25) compared to equations (3-22) and (3-23). The phase constant is not present, and A_{+} is a simpler equation of grain angle. Although simple analytical expressions for the phases measured from the system are difficult to give, the phase readings from the dipoles are also functions of grain angle, moisture content, and specific gravity, as will be shown by the experimental data later.

The moisture content effects upon the amplitude readings are not the same at different grain angles since the moisture content affects the attenuation along the grain and across the grain differently. For microwaves above 10 GHz, the attenuation is mainly controlled by moisture content [14]. As moisture content increases, the attenuation constants increase as well. Because the moisture absorption sites in wood are generally aligned with the grain direction for moisture content below saturation point, α_P increases rapidly with added moisture. The corresponding change in α_T is rather flat.

The normalized amplitude reading A_{90} in equation (3-24) can be rearranged as

$$A_{90} = \frac{\sin^2 2\theta}{4} e^{-2\alpha_T d} \left[1 + e^{-2(\alpha_P - \alpha_T)d} - 2e^{-(\alpha_P - \alpha_T)d} \cos(\beta_P d - \beta_T d) \right] \qquad (3\text{-}26)$$

For most wood species, α_P is about 1.5 to 2.5 times α_T. From earlier research work [10], $(\alpha_P - \alpha_T)d$ is much larger than 1 for thicknesses d used in practice. Under these conditions, equation (3-26) can be approximated as

$$A_{90} \approx \frac{\sin^2 2\theta}{4} e^{-2\alpha_T d} \qquad (3\text{-}27)$$

From equation (3-27), it is easily seen that grain angle can be readily obtained using A_{90}. Several points about A_{90} can be made here:

- A_{90} is independent of the microwave power. This is common to all the normalized amplitudes.
- Since the attenuation constant is mainly controlled by moisture content and does not vary significantly with specific gravity at low moisture [13], A_{90} should be only very weakly sensitive to specific gravity.
- As explained in the last section, α_T is not a strong function of moisture content for high frequency of 10 GHz or higher, A_{90} should also be only very weakly sensitive to moisture content.
- A_{90} is a periodic function of grain angle repeating every 90 degrees, and symmetric about the 45° grain direction from $\theta = 0°$ to 90°.

All the above suggests that a grain angle prediction independent of microwave power, moisture content, and specific gravity is highly possible using A_{90}. When grain angle is known, A_* and the other normalized amplitudes can be used to calculate moisture content and specific gravity. Conclusions can also be made from equations (3-21) through (3-23) and equation (3-25):

- A_0, A_{45}, A_{-45}, and A_* are periodic functions of grain angle with a common period of 180 degrees.
- The involvement of the phase constants in the normalized amplitudes is very limited compared with the effects of the attenuation constants, especially at high moisture content. This explains again that moisture content is a more significant factor in A_0, A_{45}, A_{-45}, and A_* than specific gravity, especially when moisture is relatively high.
- A_0, A_{45}, and A_{-45} have equal values at 0° grain angle. They also have equal values at 90° grain angle. They all experience greater attenuation at 0° grain than at 90° grain angle. Their dependence on grain angle grows as moisture content increases.

Though the equations discussed above match previous results and intuitions, they are just approximate models of the real case. The range of their applicability needs to be experimentally verified.

The corresponding phase measurements from the new microwave probe are denoted P_0, P_{45}, P_{-45}, and P_{90}. Closed-form expressions for these phase measurements

are not available. The features and applications of these measurements will be discussed using experimental data in the next section.

3.4 Measurements from the New Microwave Probe - Experimental

The measurement equipment is described in Section 3.1 and schematically shown in Figure 3-1. To study the dipole readings vs. grain angle, a rotating table is used to turn the wood samples in the microwave field. Dipole readings are recorded for about every degree. The rotating table is made of UHMW plastic for minimum interference to the microwave fields.

Typical wood measurements using the new microwave probe are shown in Figure 3-6 taken with a 2 by 4 Douglas-fir sample at 19% moisture content. Figure 3-6(a) shows the normalized amplitude measurements, and Figure 3-6(b) shows the measured phase changes expressed in degrees. For clarity, the measured data are shown in curves by connecting adjacent data points, instead of scattered dots. The smoothness of the curves displays the measurement consistency of the instrumentation system. Basically, all the amplitude readings are well explained using the equations provided in Section 3.3. The phase measurements also match well with theoretical expectations.

(a)

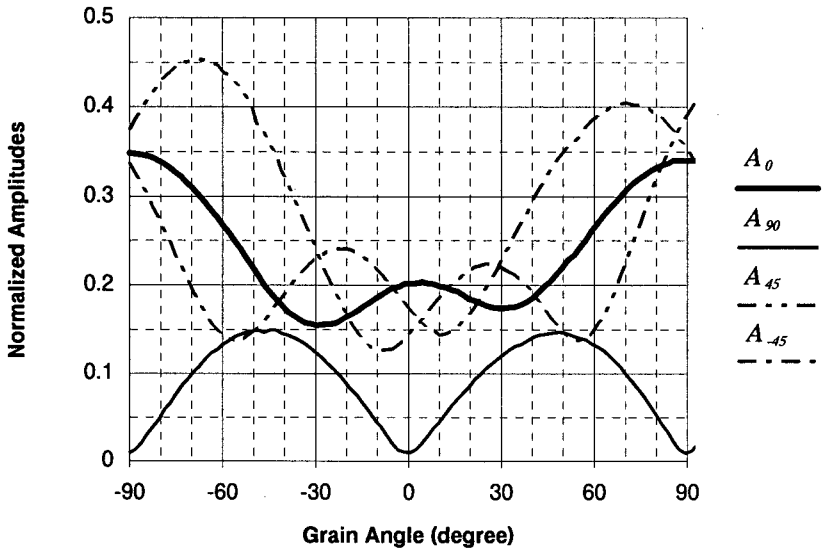

(b)

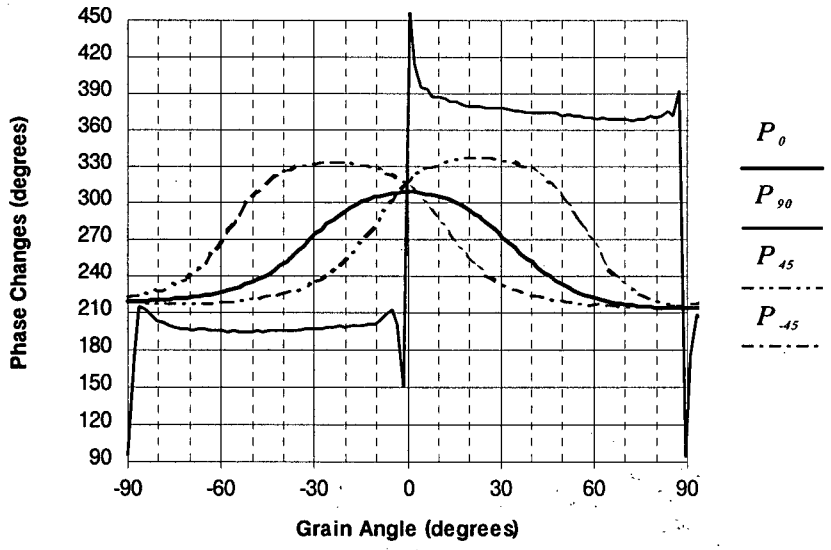

Figure 3-6 Microwave Measurements Using the New Probe

2×4 Douglas-fir at 19% MC

(a) Amplitudes (b) Phase

As predicted in equation (3-27), Figure 3-6(a) shows that measured A_{90} is very sensitive to grain angle especially when grain angle is small. By using A_{90}, grain angle can be quantified. The measurements from the two 45 degree dipoles provide criteria for determining the sign of the grain angle. From Figure 3-6(b), when grain angle is between 0° and 90°, the phase change P_{-45} is smaller than P_{45}, and the opposite for grain angle between 0° and −90°. Thus, the sign of the grain angle can be readily obtained by comparing P_{-45} and P_{45}.

When grain angle changes sign from negative to positive, the phase change measured from the 90 degree dipole, P_{90}, jumps 180 degrees, as shown in Figure 3-6(b). This can be explained by equation (3-20), which indicates that the electric field along the 90 degree dipole changes direction as grain angle changes from negative to positive. This directional change is reflected by the 180 degree jump in the P_{90} measurement. Thus P_{90} can also be used to indicate the sign of the grain angle.

The non-unique definition of A_{90} within a 90° period makes it difficult to distinguish a grain angle within 0° to 45° and one within 45° to 90°. However, grain angles greater than 20-30 degrees rarely occur in practice. Also, Hankinson's formula [2] shows that most of the strength reduction of wood occurs at smaller angles. Hence, for lumber strength grading applications, it is sufficient to assign all larger grain angles to the category "above 30 degrees".

As shown in Figure 3-6(a), the curve shapes of the amplitude measurements A_0, A_{-45}, and A_{45} match very well with equations (3-21) through (3-23) derived from the simplified theory using numerical simulations. It is clear that these measurements cannot

be represented by simple functions. The agreement between theoretical expectations and experimental measurements shows the reliability of the measurements. It also helps in the later modeling of the measurements for wood property predictions later.

The measured phase changes P_0, P_{-45}, and P_{45} in Figure 3-6(b) are also theoretically expected. Since the phase constant along the grain is much larger than across the grain, P_0 is the largest at 0° grain angle and it is the smallest when the grain angle is 90°. When the grain angle is negative, the grain direction is closer to the -45^0 dipole than to the 45^0 dipole, the -45^0 dipole sees more change in the electric field, and P_{-45} is larger than P_{45}. When the grain angle is positive, the grain direction is closer to the 45^0 dipole than to the -45^0 dipole, the 45^0 dipole sees more change in the electric field. Therefore, P_{45} is larger than P_{-45}. When the grain angle is 0 degrees, the electric field component across the grain is zero, all the dipoles measure the same electric field, i.e., the field component along the grain. This feature explains that P_0, P_{-45}, and P_{45} have the same value at 0 degree grain angle in Figure 3-6(b).

This section is only intended to illustrate the appearance of the measurements from the new probe. Detailed discussions on the prediction of wood properties are left to later chapters.

3.5 Chapter Summary and Conclusion

This chapter is a continuation of Chapter 2, which theoretically identified the need for microwave measurement of solid wood properties.

Section 3.1 described the measurement instrumentation adopted in this study. Section 3.2 introduced the design of a new microwave probe that can be used to characterize elliptically polarized microwave field which occurs when microwaves propagate through wood. Section 3.3 theoretically derived the equations of the measurements of the new probe in the presence of wood with the current instrumentation and showed the feasibility of using the new probe for measuring wood properties. Section 3.4 gave typical amplitude and phase measurements using a Douglas-fir sample. The measured data match very well with theoretical expectations. The measurements experimentally demonstrated the capability of the new probe for wood property measurements.

The close agreement between the theoretical expectation and experimental measurements displayed in section 3.2 and 3.3 shows the measurement reliability of the instrumentation system, and indicates that the theoretical derivations in sections 3.2 can be used as a guidance for data modeling and calibration in the subsequent experimental measurements.

4.0 MEASUREMENT CONSIDERATIONS

------ Answers to Often Raised Questions

4.1 Overview

This chapter addresses some of the frequently asked questions in measuring solid wood properties, such as the impact of annual ring direction, diving grain, thickness variation. The effects of temperature will be discussed in detail in Chapter 7.

Before a large number of sample is tested, it is always beneficial that a smaller number of samples be measured to check the fundamentals of the methodology, and to ensure that the equipment is working correctly.

The characteristics of the mechanical properties of wood are relatively well understood. From there, some of the questions are often raised, e.g., is there a significant strong effect from the diving grain in the microwave measurements just as in the mechanical properties? Answering these questions will allow further understanding of the microwave measurements and eliminate unnecessary concerns.

4.2 Effects of Annual Ring Direction

Figure 4-1 is a sketch of the cross section of three Douglas-fir samples with different annual ring orientations. The annual ring direction is defined as the angle between the annual ring and the lumber face. The samples all have straight grain in longitudinal direction.

The experimental samples are cut from the same wood block, and the centers of the three samples share the same annual ring. The wood block is from a large old-growth log and is cut from a position that is far from the center of the log. This ensures that the three samples made of the wood block have approximately the same physical properties. The microwave measurements from these three samples are shown in Figure 4-2. It is seen that the measurements from the three different samples are almost equal.

According to references [14-15, 28], the dielectric constants along the annual ring direction (the tangential direction) and the radial direction (perpendicular to the annual ring direction) are very close, especially at low moisture content under fiber saturation point. Therefore, the results displayed in Figure 4-2 are reasonable. The effects of the annual ring direction can be neglected.

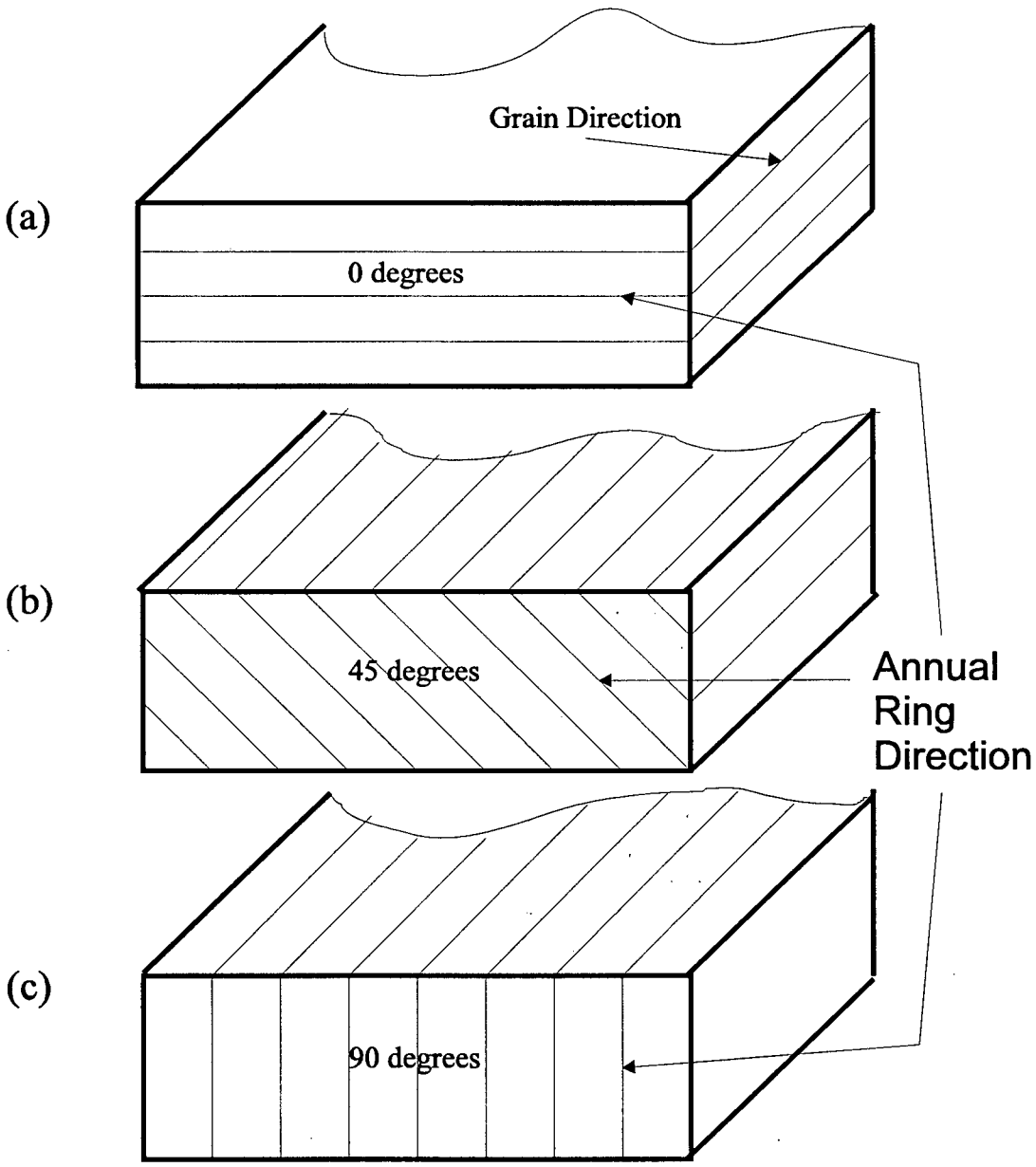

Fig. 4-1 Sketch of Cross Sections of Samples
with Different Annual Ring Direction

(a) **Annual Ring at 0 degrees**

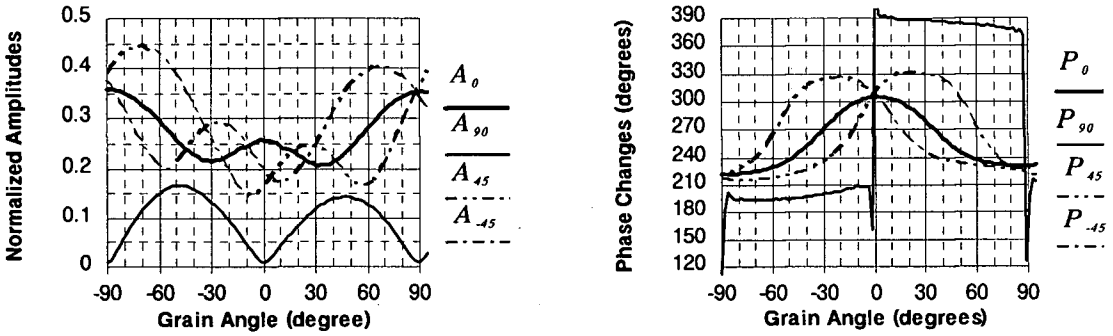

(b) **Annual Ring at 45 degrees**

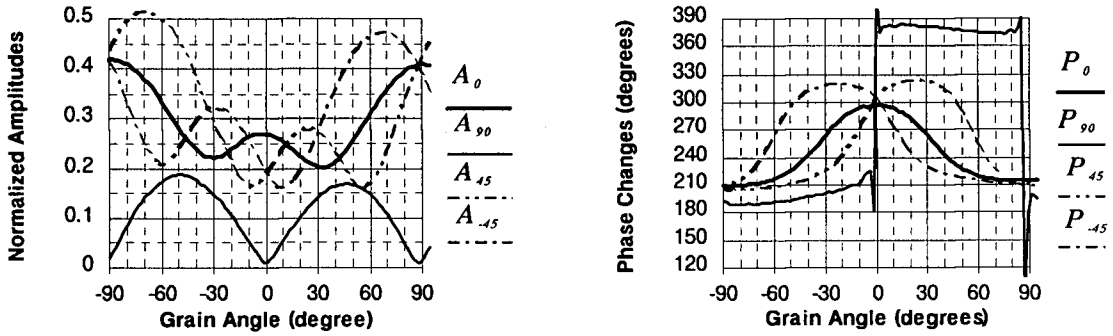

(c) **Annual Ring at 90 degrees**

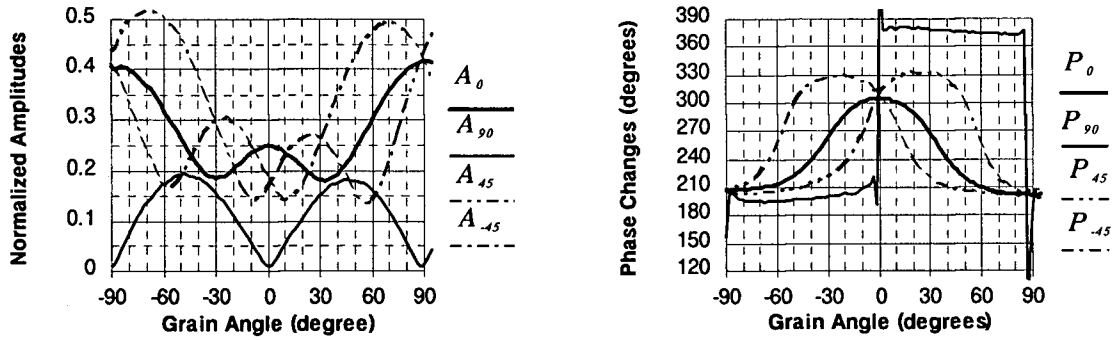

Fig. 4-2 Effects of Annual Ring Direction

4.3 Effects of Diving Grain

So far, the term "grain angle" in this thesis refers to the angle between the fiber direction and the lumber longitudinal direction in the plane of the lumber face. Diving grain is the angle between the fiber direction and the lumber face. It is caused either by the growth characteristics of the trees or by sawing. Figure 4-3 shows the sideviews of three different samples without diving grain and with 10 degree and 15 degree diving grain. The microwave measurements made from these three samples are shown in Figure 4-4.

Overall, the dielectric constant in the plane of the lumber face with the presence of diving grain is smaller than in the case without diving grain. It is therefore expected that the microwave attenuation and phase change should be smaller when there is diving grain. This is seen from Figure 4-4 by comparing the cases (a), (b), and (c). Case (c), with 15 degree diving grain, the normalized amplitudes are greater than the corresponding values in the 10 degree and 0 degree cases. Figure 4-4(a) and (b) also show that the diving grain in reasonable range does not have significant effect on the microwave measurements.

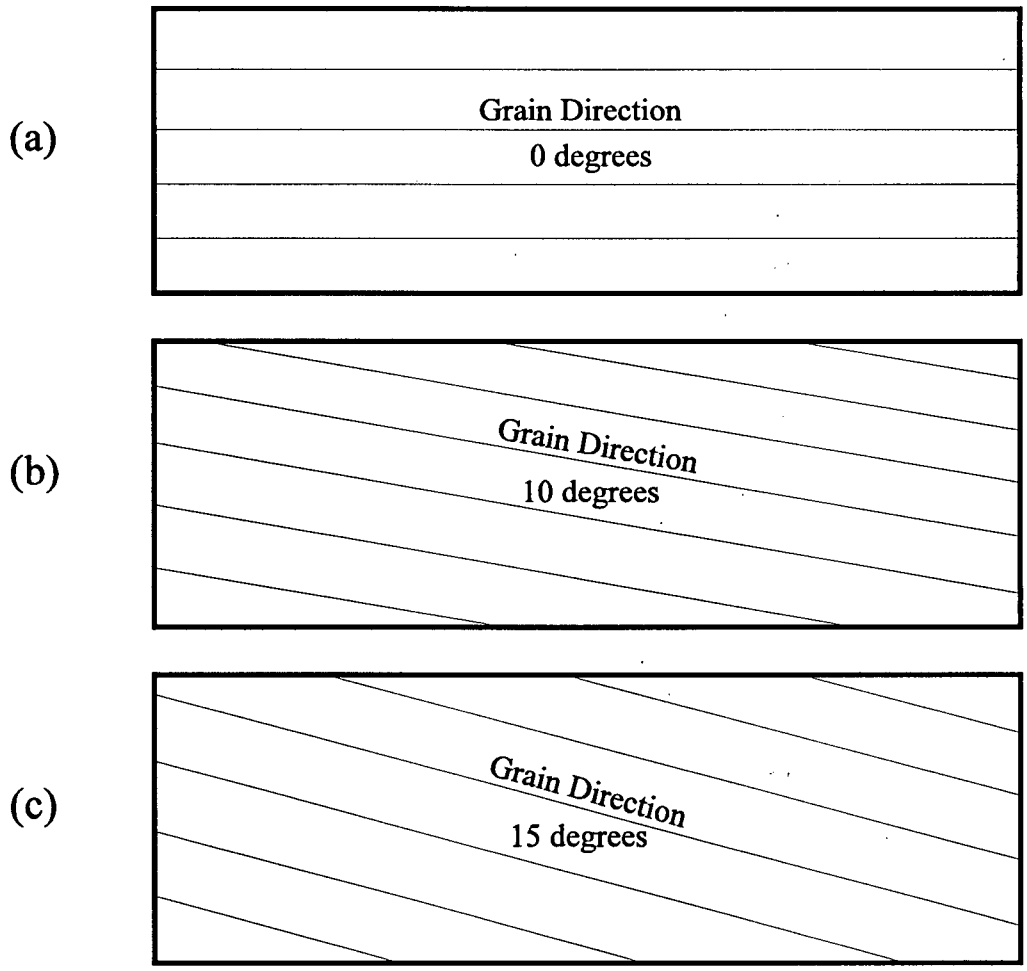

Fig. 4-3 Sideviews of Samples with Diving Grain

(a) **0 degree diving grain**

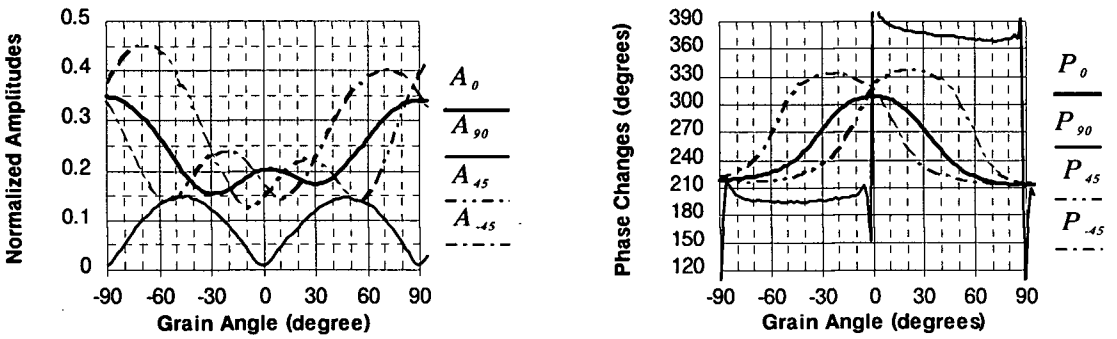

(b) **10 degree diving grain**

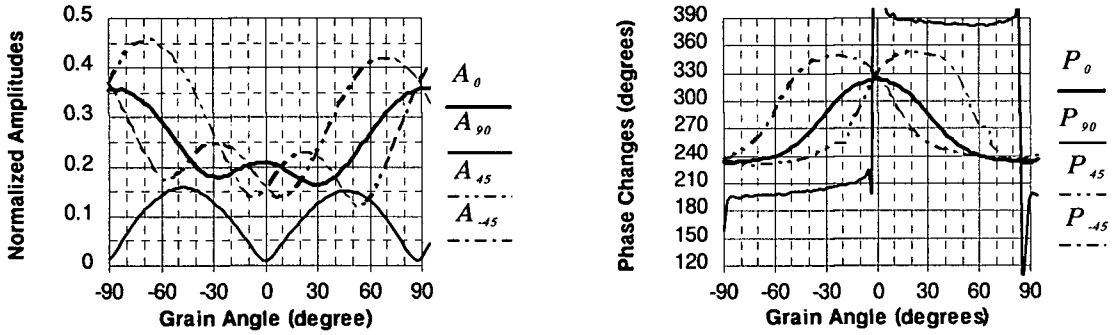

(c) **15 degree diving grain**

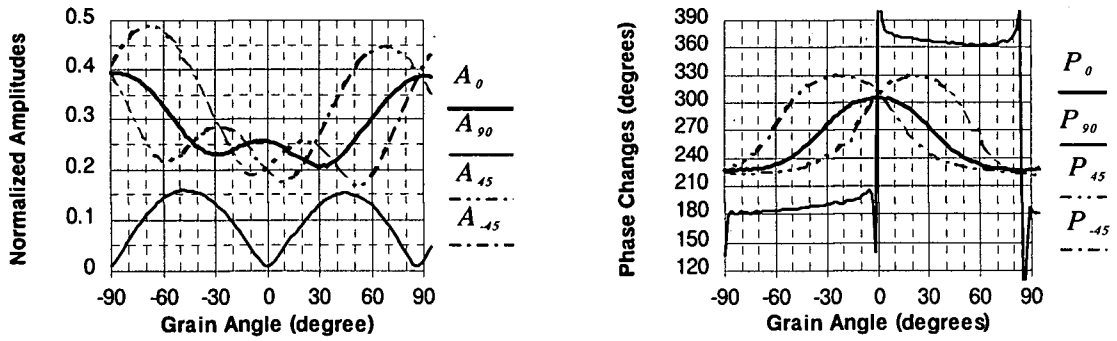

Fig. 4-4 Effects of Diving Grain

4.4 Effects of Lumber Thickness Variation

Wood specimen thickness variation is a potential concern when considering the design and performance of the microwave measurement system. Variation in specimen thickness causes changes in the amplitude and phase measurements that could be misinterpreted as indicating specific gravity and moisture content variations. To investigate this question further, some matched sets of wood specimens with uniform *SG* and *MC* were prepared. The specimens within each set had a variety of thickness. Figure 4-5 shows the microwave amplitude and phase measurements for a typical set of Douglas-fir specimens. Figure 4.6 shows the corresponding variation of some key amplitude and phase measurements with specimen thickness.

Figure 4-6(a) shows that amplitude A_0 decreases with increasing wood thickness. This behavior is caused by the increased attenuation of microwave radiation through greater wood thickness. Equation (3-21) also indicates this result. All terms in the equation are exponentially decaying and have the same sign.

In contrast, Figure 4-6(c) shows that amplitude A_{90} increases with wood thickness increase. Initially, this seems an anomalous result. However, closer study indicates that it is expected because A_{90} is a measure of depolarization as well as of attenuation. The 90 degree dipole is set perpendicular to the electric field, and in the absence of any depolarization, it returns a null measurement. This is confirmed by the theoretical result equation (3-26). Increasing thickness of off-axis dielectric material, the wood, creates depolarization and thereby increases A_{90}. Eventually, the microwave depolarization

reaches a maximum. Further wood thickness increase merely increases attenuation, and A_{90} starts to fall.

Figure 4-6(c) shows the initial increase in A_{90}. The subsequent decrease occurs at much larger wood thickness. The theoretical expression of A_{90} equation (3-26) also describes this behavior. The equation contains exponentially decaying terms, but some have positive signs, and others negative signs. At very small specimen thickness, the opposite sign terms cancel, and A_{90} is close to zero. With increasing wood thickness, the positive term representing the field across the grain direction decays slower than the negative terms and A_{90} rises. However, all the terms decay exponentially, and so eventually A_{90} peaks and decreases back towards zero.

Figure 4-6(b) also shows that the measured phase increases approximately linearly with specimen thickness. Thus, it is seen that all amplitude and phase measurements vary approximately proportionally and inversely proportionally with wood thickness, or some variation between. Their absolute slopes are typically less than one. Therefore, the percentage amplitude or phase change caused by say 1% change in wood thickness is within the range from -1% to 1%. In sawmills, lumber is planed under well-controlled conditions, and the thickness variation of newly planed material is typically within 1%. Thus, for practical applications, the variation in microwave readings caused by wood thickness variations is not excessive, and can generally be ignored, for a given nominal thickness.

(a) **Thickness= 1.2cm**

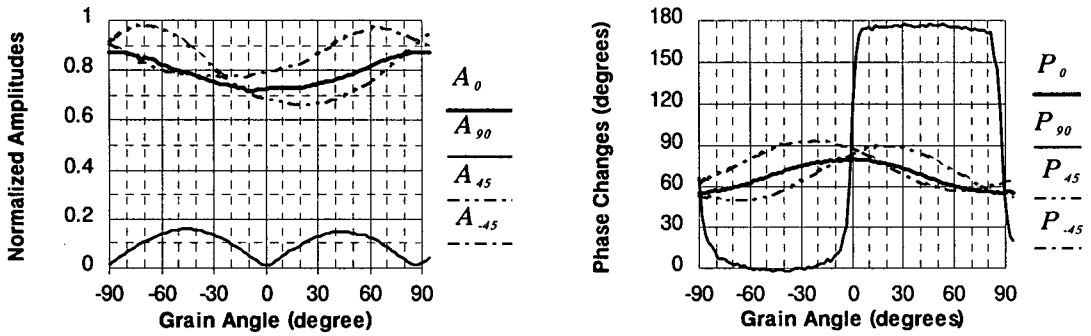

(b) **Thickness= 2cm**

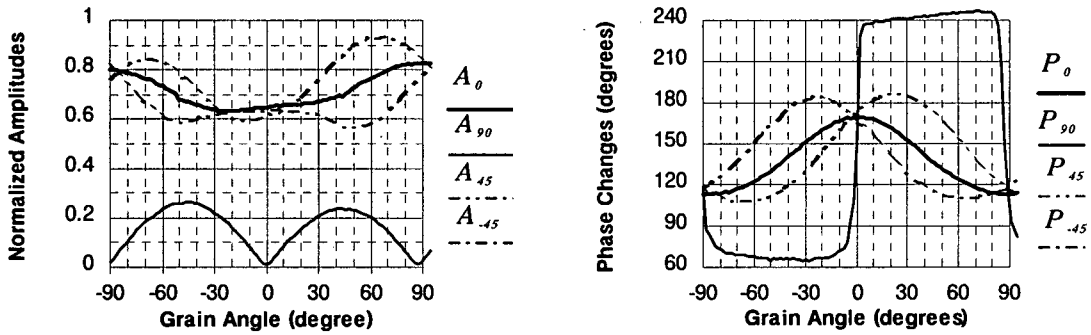

(c) **Thickness= 3cm**

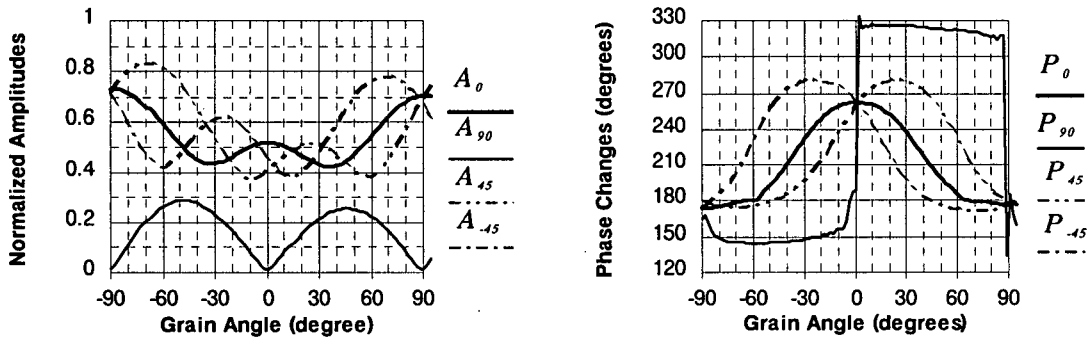

Fig. 4-5 Specimen Thickness Effect in Microwave Amplitude and Phase Measurements from Matched Douglas-fir Specimens
(a) Thickness = 1.2cm (b) Thickness = 2 cm (b) Thickness = 3cm

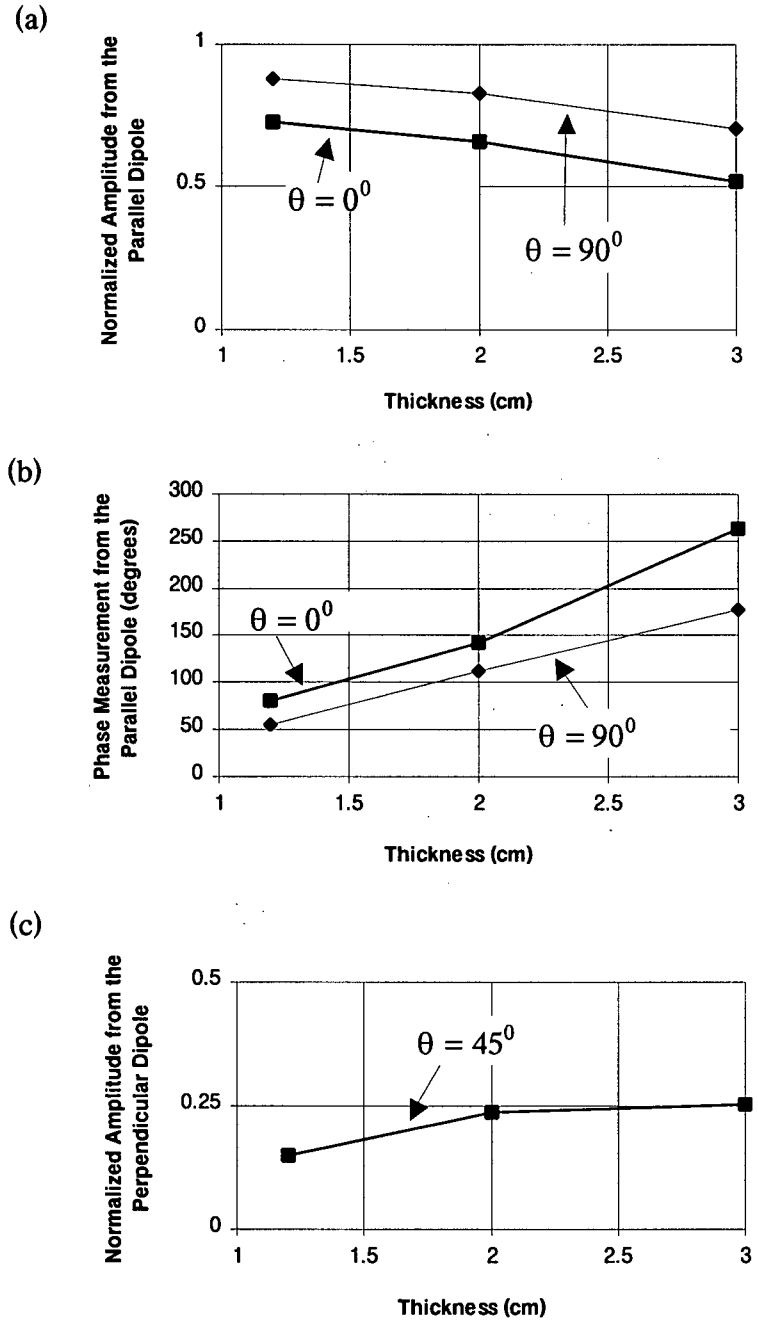

Fig. 4-6 Specimen Thickness Effect in Microwave Amplitude and Phase Measurements from Matched Douglas-fir Specimens

(a) Amplitude A_0 at $\theta = 0°$ and $\theta = 90°$

(b) Phase P_0 at $\theta = 0°$ and $\theta = 90°$

(c) Amplitude A_{90} at $\theta = 45°$

4.5 Chapter Conclusion

This chapter investigated the effects of various wood structural characteristics on the microwave measurements. It is found that the wood annual ring direction has no significant effect on the microwave measurements, and nor does small diving grain up to about 15°. It is also found both theoretically and experimentally that small thickness variation in dimension lumber, typically 1%, does not greatly affect the microwave measurements. These factors need not be given consideration in the procedures for determining the grain angle, specific gravity, and moisture content discussed later on.

5.0 GRAIN ANGLE EVALUATION USING MICROWAVE MEASUREMENTS

5.1 Chapter Overview

The previous chapters have established the foundation of using microwave measurements for determining wood properties. This chapter focuses on the use of microwave measurements to identify grain angle.

As stated in the "Introduction", grain deviation is a major strength controlling characteristic in lumber. Thus, the ability to measure grain angle in real time is a critical step when developing an improved lumber strength grading system.

The results of the theoretical analysis in Chapter 3 will be directly used to create a working model of the experimental data. Even though the microwave changes after transmission through wood are dependent on the wood specific gravity and moisture content, it will be shown that grain angle evaluation can be made independent of the specific gravity and moisture content. This can be done by carefully choosing information from the abundant microwave measurements and by proper modeling.

The experimental microwave measurements described in section 3.4 show that each of the measurements from the four-dipole sensor in Figure 3-5 vary with the grain angle. The amplitude measurement from the perpendicular dipole, A_{90}, shown in Figure 3-6, has the simplest form and varies most strongly with the grain angle. The greatest grain angle sensitivity occurs in the range up to 30 degrees. This feature allows the use of

A_{90} as a sensitive indicator of the grain angle up to 30 degrees. This range is sufficient for strength grading, because most strength reduction due to grain deviation in wood occurs in the small grain angle range less than 20 degrees. All the other measurements vary less significantly with the grain angle, and they have more complicated forms. But they are useful to compensate the variations in A_{90} due to other factors, such as specific gravity and moisture content, as will be discussed in this chapter.

5.2 Sample Wood Specimens

In the following sections, various sets of measurements will be described, aimed at identifying the relationship between the wood physical properties and the microwave measurements. To achieve consistent and reliable measurements, a set of sample wood specimens was carefully prepared. These specimens were used for most measurements.

The wood sample set consisted of one hundred specimens, fifty of them Douglas-fir, and fifty spruce. The mixture of species was chosen both to allow examination of any species-dependent effects, and also to provide a wide range of specific gravity. The samples were nominal $2'' \times 4''$ lumber blocks, about $6''$ long. They were initially stored in various conditioning rooms for one to two months so that they could reach equilibrium moisture content. The resulting moisture contents were in the range of 8% to 17% dry basis.

To preserve the moisture in the samples during the test period, the ends of the samples were painted with plastic paint, and the samples were further sealed in 2-mil plastic bags.

The wood specimens were chosen so that they contained only straight, uniform grain. The grain direction in each sample relative to its length was determined using a Metriguard slope-of-grain indicator. This angle was used to establish the datum for the microwave grain angle measurements.

At the conclusion of all the microwave measurements, the sample dimensions and weights were recorded. The samples were then oven dried at $106\,^{\circ}C$ for 24 hours, and re-weighed. These data provided gravimetric measurements of the moisture content and dry-basis specific gravity of each of the samples. The resulting set of grain angle, specific gravity, and moisture content data serve as the reference data against which the various microwave measurements are compared.

5.3 Grain Angle Evaluation Using A_{90} and Model Selection

From the simplified theory presented in Section 3.3, the amplitude of the perpendicular dipole A_{90} can be expressed by equation (3-27), here reprinted as equation (5-1),

$$A_{90} \approx \frac{\sin^2 2\theta}{4} e^{-2\alpha_T d} \tag{5-1}$$

From this equation, the grain angle can be explicitly expressed using A_{90}, namely,

$$\begin{aligned} \theta &= \frac{1}{2}\sin^{-1}\left(2\sqrt{A_{90}}e^{\alpha_T d}\right) \text{ (radians)} \\ &= \frac{90}{\pi}\sin^{-1}\left(2\sqrt{A_{90}}e^{\alpha_T d}\right) \text{(degrees)} \end{aligned} \tag{5-2}$$

where the term $\sqrt{A_{90}}$ is the measured quantity and $e^{\alpha_T d}$ describes the material characteristics. The attenuation constant across the grain α_T does not vary significantly with the moisture content and specific gravity. Thus, as a first approximation, the term $e^{\alpha_T d}$ in equation (5-2) can be approximated as a constant. Then, a simple regression model for grain angle θ is proposed as

$$\hat{\theta} = a_0 \sin^{-1}\left(a_1\sqrt{A_{90}}\right) \tag{5-3}$$

where $\hat{\theta}$ is the estimated grain angle. Parameters a_0 and a_1 directly replace the coefficients in the theoretical expression of θ in equation (5-2). Their theoretical values are $90/\pi$ and $e^{\alpha_T d}$. The theoretical values of the parameters can be employed as the initial values in a non-linear regression.

An experiment was conducted to provide grain angle regression data. One hundred samples, half of them Douglas-fir and half spruce, were measured. Following the method described in Chapter 4, amplitude and phase measurements were taken at

about 1.5 degree intervals while the wood samples were rotated in the microwave field within the range of -30 degrees to 30 degrees.

Equation (5-3) is incapable of distinguishing negative and positive grain angles. Therefore, the absolute value of the grain angle is used. A non-linear regression over the data collection gives a moderate coefficient of determination of $r^2 = 0.88$, and a standard error of 2.96 degrees. The estimated parameters are

$$a_0 = 22.92; \quad a_1 = 2.01. \tag{5-4}$$

To improve regression performance, the model in equation (5-3) is relaxed to

$$\hat{\theta} = b_0 \sin^{-1}\left(b_1 A_{90}^{n}\right) \tag{5-5}$$

The introduction of n is to allow for the approximation in the simplified theory. A new regression using the same experimental data gives an improved coefficient of determination of $r^2 = 0.94$ and a standard error of 2.06 degrees. The estimated parameters are

$$b_0 = 433.23; \quad b_1 = 0.27; \quad n = 0.88. \tag{5-6}$$

The higher coefficient of determination and lower root mean square of error make this model quite attractive. Though the increased accuracy is based on added complexity and deviation from the physical model, the new model is still quite simple.

High material throughput rates in sawmills require that practical grain angle measurement systems be able to run at high speeds. Therefore the grain angle measurement model that is used must be as simple as possible. For small grain angles, it is reasonable to assume that

$$\sin\theta \approx \theta \tag{5-7}$$

Thus, model equation (5-5) can be simplified to

$$\hat{\theta} = c_1 A_{90}^{n} \tag{5-8}$$

Regression of model equation (5-8) over the same data collection gives a coefficient of determination of 0.94 and a standard error of 2.05 degrees. The estimated parameters are

$$c_1 = 121; \quad n = 0.91. \tag{5-9}$$

Hence, the resulting equation for grain angle evaluation is

$$\hat{\theta} = 121 A_{90}^{0.91} \text{ (degrees)} \tag{5-10}$$

The regression results of model (5-8) and (5-5) are almost the same. Model (5-8) has fewer parameters and simpler form compared to model (5-5), thereby making it a better choice.

Fig. 5-1 shows the result of applying equation (5-10) to the original data for the one hundred samples. The scattered circles show that the evaluation is more accurate for smaller grain angles. This occurs because the slope of the A_{90} vs. grain angle curve, such as shown in Figure 3-6(a), is largest at small grain angles. The moderate standard error of 2.05 degrees shows that the current system is effective in determining grain direction. But improvement is desirable. The above discussion is based on A_{90} measurement alone without accounting for the effects of wood moisture content and specific gravity. An improved result may be achieved by combining other measurements into the regression model.

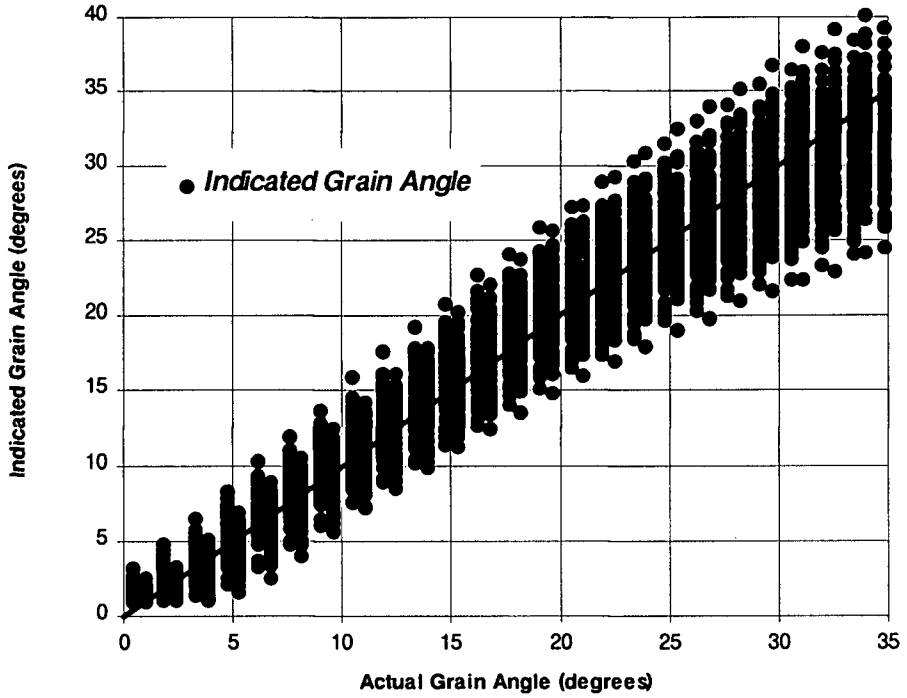

Fig. 5-1 Grain Angle Identification Using the Amplitude Measurement of the Perpendicular Dipole A_{90} with Equation (5-10)

5.4 Grain Angle Evaluation Using A_{90} and the Phase Measurements

In Section 3.4, it was shown that the phase measurements from the two 45 degree dipoles can identify the sign of the grain angle. When the grain angle is less than 0 degrees, the phase change measured from the -45 degree dipole is larger than that measured from the 45 degree dipole. Conversely, when the grain angle is positive, the phase change measured from the -45 degree dipole is smaller than that measured from the 45 degree dipole. In Figure 3-6, a slight asymmetry exists in the measurements. This asymmetry is mainly due to minor misalignments in the microwave measurement system. When non-linear regressions are performed on the absolute values of the grain angles, the asymmetry in the measurements causes larger error. Knowing the sign of the grain angles, the regressions can be done for negative angles and positive angles separately.

In the last section, model (5-8) was suggested because of its simplicity and effective performance. The added information of grain angle sign allows inclusion of a constant term into the right hand side of model (5-8) to account for the misalignments in the measurement system. The new model is then,

$$\hat{\theta} = c_0 + c_1 A_{90}^n \tag{5-11}$$

For negative grain angles, the regression gives a coefficient of determination of 0.95, and a root mean square of error of 1.86 degrees. The estimated parameters are

$$c_0 = 0.77;\ \ c_1 = -116.9;\ \ n = 0.89. \tag{5-12}$$

The equation for grain angle estimation is

$$\hat{\theta} = 0.77 - 116.9 A_{90}^{0.89} \tag{5-13}$$

The results of applying equation (5-13) to the original data is shown in Figure 5-2.

For positive grain angle, the regression results a coefficient of determination of 0.95, and a root mean square of error of 1.93 degrees. Again, substituting the estimated parameters into equation (5-11) gives the equation for grain angle evaluation, i.e.,

$$\hat{\theta} = -0.14 + 122.9 A_{90}^{0.89} \tag{5-14}$$

Figure 5-3 shows the evaluated grain angle versus the measured grain angle using equation (5-14).

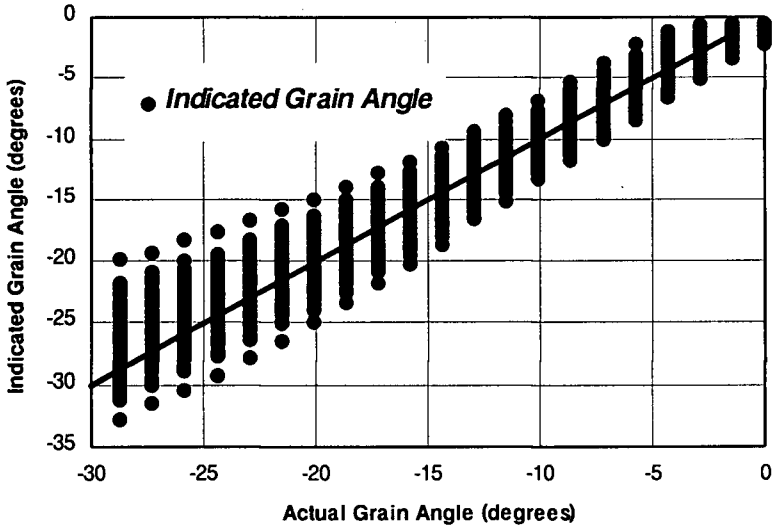

Fig. 5-2 Negative Grain Angle Identification Using the Amplitude Measurement from the Perpendicular Dipole with Equation (5-13)

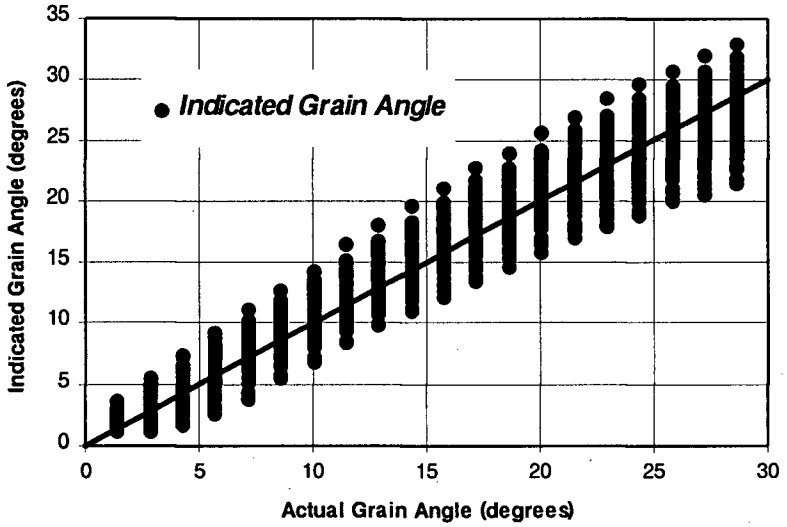

Fig. 5-3 Positive Grain Angle Identification Using the Amplitude Measurement from the Perpendicular Dipole with Equation (5-14)

5.5 Grain Angle Evaluation Using A_{90} and the other Amplitude Measurements

A coefficient of determination of $r^2 = 0.95$ is a very impressive number considering that wood is a natural material. However, it is desirable to improve the standard error of 1.86 degrees for negative grain angles and 1.93 degrees for positive grain angles.

Generally, some of the variations in the grain angle identification are caused by the variations in the A_{90} measurements due to the changes in moisture content and specific gravity. These effects are expressed by the term $e^{\alpha_T d}$ in equation (5-1). From

the theoretical analysis in Chapter 3, all the measurements are functions of $e^{\alpha_T d}$. Therefore, $e^{\alpha_T d}$ can be modeled by using the microwave measurements. Because the A_{90} measurement alone is responsible for 95% of the variations in the grain angle evaluation, it is not necessary to add more parameters to account for the last 5% percent of the variations. Hence, only simple modifications to model (5-11) is considered.

Microwaves experience greater attenuation at higher moisture content. Basically, all the amplitude measurements decrease as moisture content increases. The specific gravity has similar effects to the amplitude measurements, but not as strong. But the effects of moisture content and specific gravity on A_{90} is much smaller than on the other amplitude measurements because $e^{\alpha_T d}$ varies less significantly with moisture content and specific gravity than $e^{\alpha_P d}$ does. Therefore, direct use of the other amplitude measurements in equation (5-11) will over-compensate the moisture effect in the A_{90} measurements.

Moisture content has a smaller influence on $A_* = (A_{-45} + A_{45})/2$ than on A_0. Therefore, the ratio A_*/A_0 carries less moisture influence than the individual measurements, but still contains moisture information. Hence, multiplying the term A_*/A_0 with the measurement term in model (5-11) may yield some improvement. A revised model based on equation (5-11) is then proposed as

$$\hat{\theta} = c_0 + c_1\left(A_{90}\frac{A_*}{A_0}\right)^n \tag{5-15}$$

For negative grain angles, the regression gives a slightly improved coefficient of determination of 0.96, and a standard error of 1.69 degrees. The resulting model equation is

$$\hat{\theta} = 1.6 - 89\left(A_{90}\frac{A_*}{A_0}\right)^{0.73} \tag{5-16}$$

The results of applying equation (5-16) to the original data is shown in Figure 5-4.

For positive grain angles, the regression also results in some improvement, a coefficient of determination of 0.95, and a standard error of 1.78 degrees. Again, substituting the estimated parameters into equation (5-15) gives the equation for grain angle evaluation, i.e.,

$$\hat{\theta} = -1.1 + 98\left(A_{90}\frac{A_*}{A_0}\right)^{0.74} \tag{5-17}$$

Figure 5-5 shows the evaluated grain angle versus the measured grain angle using equation (5-17).

Notice that the 0.95 coefficient of determination from model (5-11) is quite high, and so any significant improvement is difficult. The extra amplitude measurements used in model (5-14) are useful for determining specific gravity and moisture content. Thus, the adoption of model (5-14) in place of model (5-11) does not pose extra measurement effort.

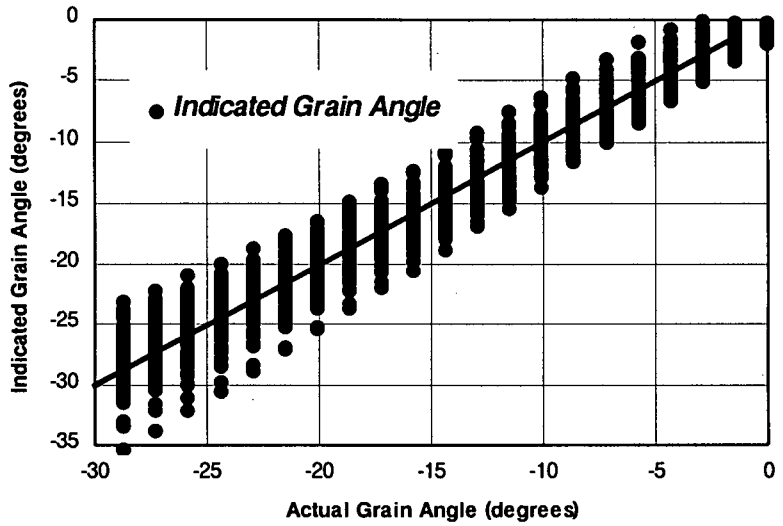

Fig. 5-4 Negative Grain Angle Identification Using the Amplitude Measurements from all Dipoles with Equation (5-16)

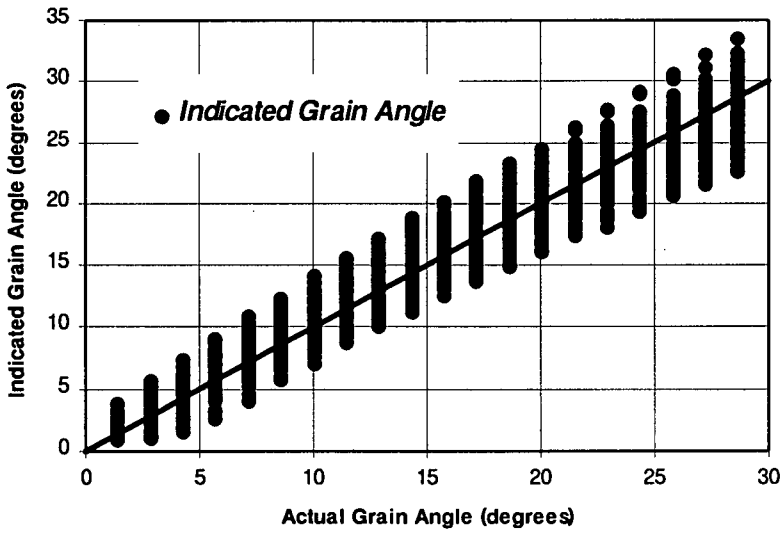

Fig. 5-5 Positive Grain Angle Identification Using the Amplitude Measurements from all Dipoles with Equation (5-17)

5.6 Chapter Conclusion

This chapter discussed the use of microwave measurements for determining wood grain angle. The theoretical analysis developed in Chapter 3 provided the basis for the modeling of the experimental measurements. Using model equation (5-8), the perpendicular dipole amplitude measurement A_{90} explains 94% of the variation in grain angle measurement. With the help of the phase measurements and the amplitude measurements from the other dipoles, the coefficient of determination for grain angle evaluation reaches 96%, with a standard error of about 1.7 degrees for grain angles up to 30 degrees.

6.0 SPECIFIC GRAVITY AND MOISTURE CONTENT ESTIMATION USING MICROWAVE MEASUREMENTS

6.1 Chapter Overview

In addition to the effects of grain angle, specific gravity and moisture content also strongly influence lumber strength. The previous chapter described how wood grain angle can be determined from microwave measurements using a four-dipole scatterer and the homodyne system. This chapter discusses how wood specific gravity and moisture content can be determined from the same type of measurements.

The experimental microwave transmission measurements discussed in section 3.4 show that the measurements from the different dipoles all vary with grain angle, specific gravity, and moisture content. Specific gravity and moisture content are scalar quantities, and do not depend on grain angle. Therefore, the microwave measurements that have the least dependence on grain angle and the greatest dependence on specific gravity and moisture content will be the most useful for determining these two quantities. The amplitude and phase measurements from the parallel dipole, A_0 and P_0, are most heavily influenced by the specific gravity and moisture content. They will be the center in the data modeling for specific gravity and moisture content.

One intrinsic difficulty in using the current measurement system to extract specific gravity and moisture content information is that all the microwave measurements

are dependent on the grain angle. The mathematical models for determining the specific gravity and moisture content, thus, have to compensate for this undesirable feature in the microwave measurements to ensure that the predicted results are independent of grain angle.

6.2 Sample Experimental Observations

Figures 6-1 and 6-2 shows the microwave amplitude and phase measurements vs. grain angle from three typical Douglas-fir samples with different moisture contents. The samples have approximately equal specific gravity. For clarity, only the measurements from the parallel dipole A_0 and P_0 are shown in Figure 6-1. The measurements from the two 45 degree dipoles A_{-45}, A_{45}, P_{-45}, and P_{45} along with the average amplitude $A_* = (A_{45} + A_{-45})/2$ are shown in Figure 6-2. It is seen that the moisture content has major effects on both the amplitude and phase measurements. The attenuation and phase constants both increase with increase in moisture content. Correspondingly, the amplitude becomes smaller and the phase change becomes larger.

The effect of the specific gravity can be seen from Figure 6-3. Figure 6-3 shows the microwave measurements from three Douglas-fir samples. The three samples have about the same moisture content, but different specific gravity. The specific gravity and moisture content are dry-basis values. This is true throughout this thesis. The experimental data demonstrate that the specific gravity has significant impact on the phase measurements but a relatively small effect on the amplitude measurements at low moisture.

(a)

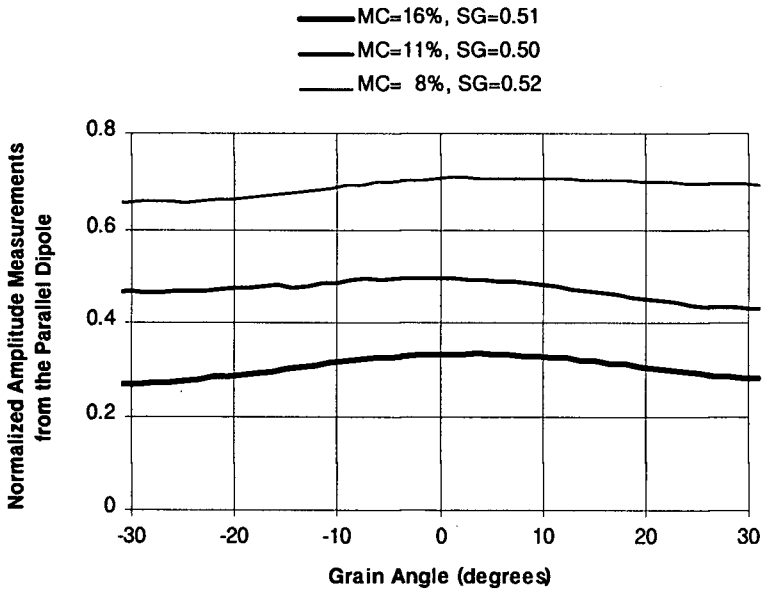

(b)

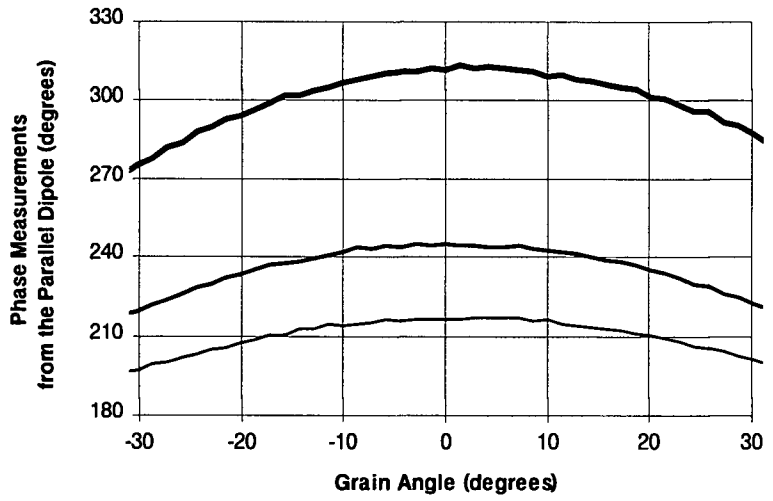

Fig. 6-1 Microwave Measurements vs. Grain Angle for a Range of Moisture Content

(a) Microwave Amplitude, A_0

(b) Phase Change, P_0

(a)

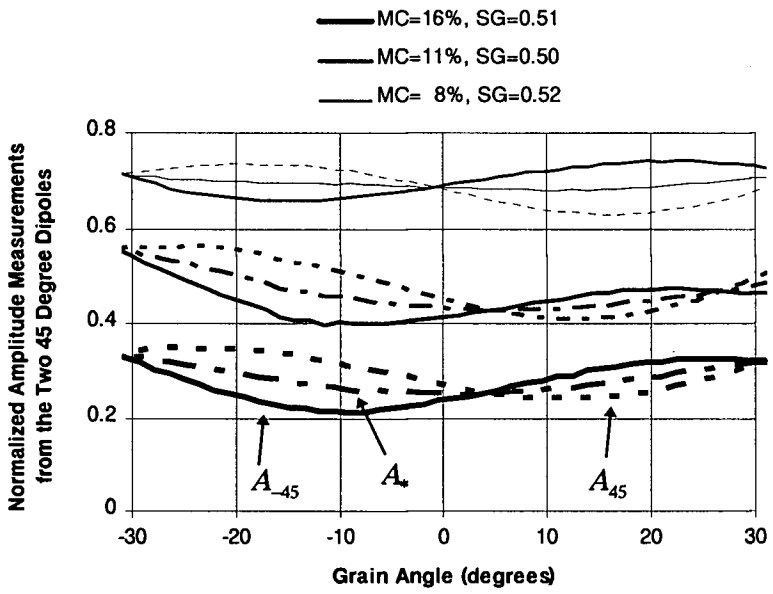

(b)

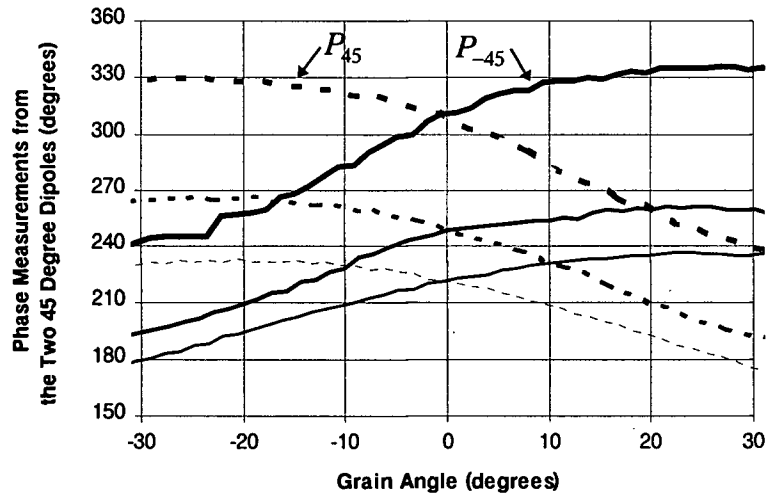

Fig. 6-2 Microwave Measurements vs. Grain Angle for a Range of Moisture Content

(a) Microwave Amplitude, A_{-45}, A_{45}, and A_*

(b) Phase Change, P_{-45} and P_{45}

(a)

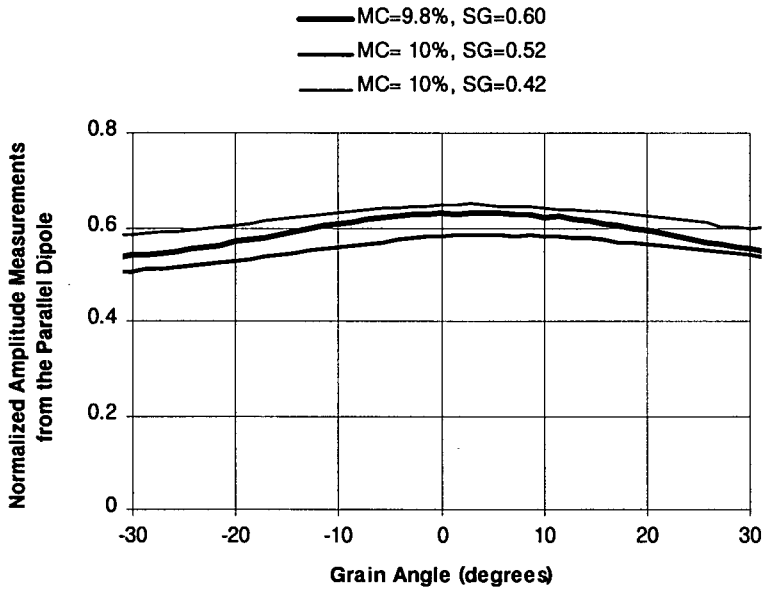

(b)

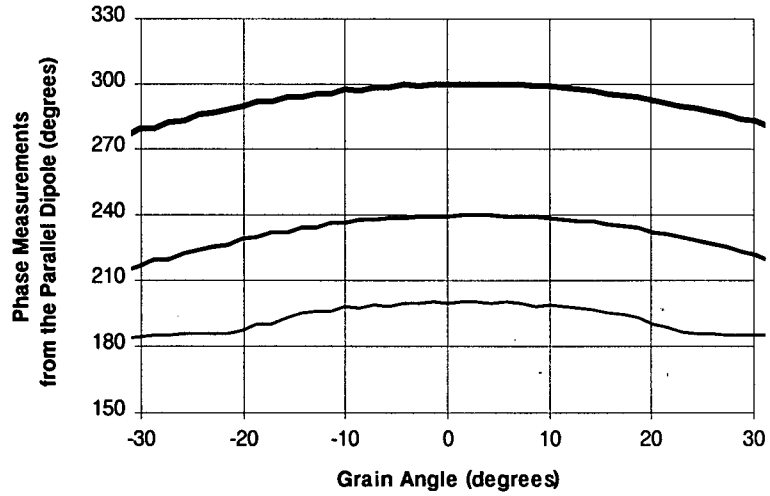

Fig. 6-3 Microwave Measurements vs. Grain Angle for a Range of Specific Gravity
(a) Microwave Amplitude, A_0
(b) Phase Change, P_0

Figure 6-2 shows that A_*, the average of A_{-45} and A_{45}, has much less curved shape than either individual amplitude measurements. Figures 6-1 and 6-2 show that both A_0 and A_* have quite similar shapes, but with A_0 curving downward and A_* curving upward. Therefore, their average may yield a grain angle independent quantity which physically retains the amplitude information. This combined quantity can be written as

$$\overline{A} = \frac{1}{2}(A_0 + A_*) \tag{6-1}$$

i.e.,

$$\overline{A} = \frac{1}{2}\left[A_0 + \frac{1}{2}(A_{45} + A_{-45}) \right] \tag{6-2}$$

Figure 6-4 shows the $\overline{A}$ curves for the same sample measurements used in Figures 6-1 and 6-2. The curves show that $\overline{A}$ is almost insensitive to changes in grain angle over the range -30° to 30°. It is therefore a good candidate for a microwave measurement to be used to indicate moisture content without explicit knowledge of grain angle.

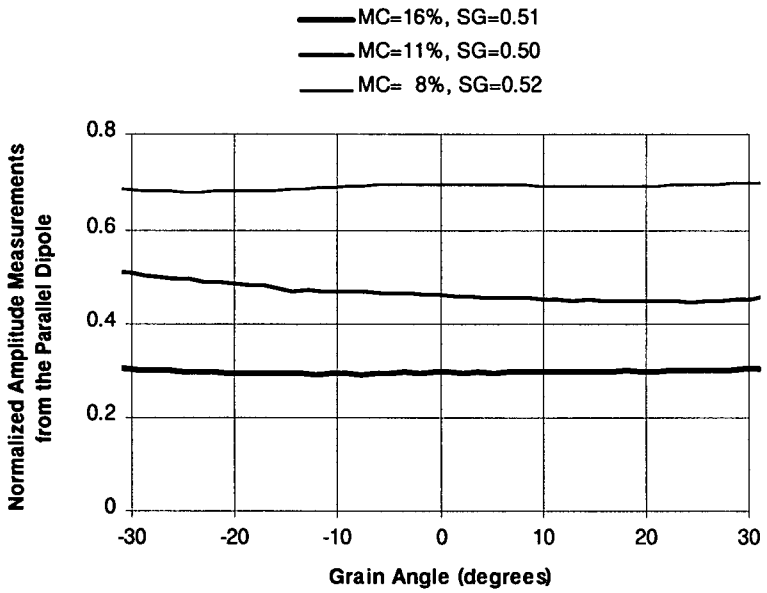

Fig. 6-4 Microwave Amplitude $\overline{A} = \left[A_0 + (A_{45} + A_{-45})/2\right]/2$ vs. Grain Angle for a Range of Moisture Content

The various phase measurements were also examined to try to identify a combination that would provide grain angle insensitive phase change information. Unfortunately, the average of the phase measurements from the two 45 degree dipoles, $P_* = (P_{-45} + P_{45})/2$, turns out to be almost identical to the phase measurement from the parallel dipole, P_0, as shown in Figure 6-5. Therefore, P_* contains no extra information. A phase quantity, analogous to $\overline{A}$, which is insensitive to grain angle, therefore cannot be formulated using the phase measurements alone. A different approach has to be taken.

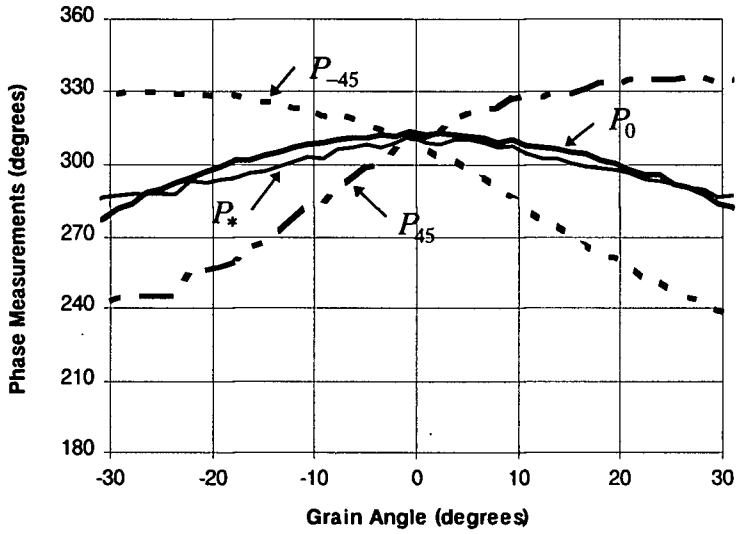

Fig. 6-5 Microwave Phase Measurements vs. Grain Angle for a Range of Moisture Content

Figure 6-1 shows that P_0 has an approximate cosine shape. It is found that the quantity

$$\overline{P} = \frac{P_0}{\cos\theta} \tag{6-3}$$

varies less significantly with grain angle than P_0 does. Figure 6-6 shows the $\overline{P}$ curves for the three Douglas-fir sample measurements based on the actual grain angle measurements, θ. The phase quantity $\overline{P}$ maintains all the phase change information

contained in P_0. It is therefore useful for obtaining grain angle independent evaluation of the specific gravity and moisture content.

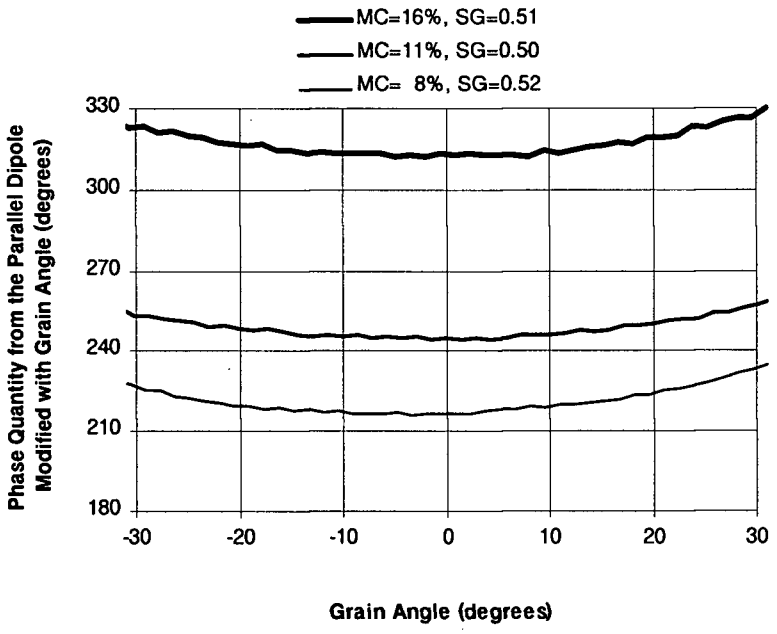

Fig. 6-6 Phase Quantity $\overline{P}$ Calculated with the Actual Grain Angle for a Range of Moisture Content

In practice, the actual grain angle θ is not available, so the estimated grain angle $\hat{\theta}$ must be used in equation (6-3), i.e.,

$$\overline{P} = \frac{P_0}{\cos\hat{\theta}} \tag{6-4}$$

From Chapter 5, the most simplified equation that can be used to identify grain angle is equation (5-8), reproduced here as equation (6-5)

$$\hat{\theta} = 121 A_{90}^{0.91} \quad \text{(degrees)} \tag{6-5}$$

This simplified equation is satisfactory here because it is not necessary to distinguish the sign of the grain angle. After substituting equation (6-5) into equation (6-4), $\overline{P}$ can be expressed as

$$\overline{P} = \frac{P_0}{\cos\left(121 A_{90}^{0.91}\right)} \tag{6-6}$$

Figure 6-7 shows the $\overline{P}$ curves corresponding to equation (6-6). The curves in Figure 6-7 have similar shape to those in Figure 6-6. Fortuitously, the errors introduced by using the estimated grain angle $\hat{\theta}$ in place of the actual grain angle θ in equation (6-4) has the effect of further decreasing the sensitivity to grain angle. Hence, equation (6-6) will be used later as a grain angle insensitive phase quantity for determining the specific gravity and moisture content.

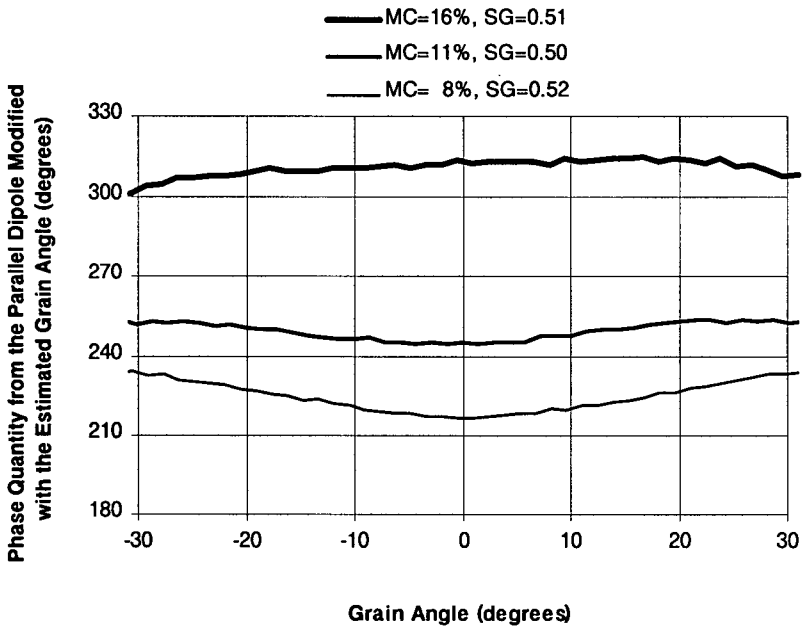

Fig. 6-7 Phase Quantity $\overline{P}$ Calculated with the Estimated Grain Angle for a Range of Moisture Content

6.3 Models for Determining the Specific Gravity and Moisture Content

The modeling of the specific gravity and moisture content can be initiated based on the simplified theory presented in Chapter 3. From Equations (3-21) to (3-23), the normalized amplitude measurements can be expressed as linear functions of the specific gravity (*SG*) and the moisture content (*MC*) if we assume a linear relationship between the dielectric constants and *SG* and *MC*. As Figure 6-4 and Figure 6-7 show, $\overline{A}$ and $\overline{P}$

do not vary substantially with the grain angle. Therefore, the use of $\overline{A}$ and $\overline{P}$ effectively eliminates the complexity caused by variations in grain angle.

King and Basuel [19] pointed out that the amplitude and phase change of the microwaves propagated through wood are highly linear with the basis weight (mass per unit area) of the wood and moisture contained in the wood. Hence, the amplitude measurement and the phase change can be expressed as

$$\overline{A} = a_1 w_d + a_2 w_w \tag{6-3}$$

and

$$\overline{P} = a_3 w_d + a_4 w_w \tag{6-4}$$

where w_d is the dry wood weight, w_w is the weight of the water contained in the wood, a_1, a_2, a_3, a_4 are material constants. Solving equations (6-3) and (6-4) simultaneously gives

$$w_d = \frac{a_4\overline{A} - a_2\overline{P}}{a_1 a_4 - a_2 a_3} \quad (\mathrm{g/cm^2}) \tag{6-5}$$

$$w_w = \frac{a_3\overline{A} - a_1\overline{P}}{a_2 a_3 - a_1 a_4} \quad (\mathrm{g/cm^2}) \tag{6-6}$$

The moisture content based on dry density is then

$$MC = \frac{w_w}{w_d} = \frac{a_3\overline{A} - a_1\overline{P}}{a_2\overline{P} - a_4\overline{A}} \times 100\% \qquad (6\text{-}7)$$

A desirable feature here is that MC as determined by Equation (6-7) is independent of thickness. The specific gravity is obtained simply by dividing Equation (6-5) by the wood thickness d, i.e.,

$$SG = \frac{a_4\overline{A} - a_2\overline{P}}{(a_1a_4 - a_2a_3)d} \qquad (6\text{-}8)$$

Equations (6-7) and (6-8) will serve as the starting point for modeling the specific gravity and moisture content in the following sections.

6.4 Specific Gravity Determination

Model Equation (6-6) can be simplified as

$$SG = b_1\overline{A} + b_2\overline{P} \qquad (6\text{-}9)$$

where b_1 and b_2 are the corresponding combinations of the coefficients a_1, a_2, a_3, a_4, and d from equation (6-8). In practice the material thickness d is constant, and so it is convenient to absorb this factor into the coefficients b_1 and b_2. To allow $\overline{A}$ and $\overline{P}$ to have about the same scale, $\overline{P}$ will be expressed in radians in the calculations, instead of

degrees. This will give both the amplitude and phase measurements about equal weight in the regressions. A simple linear regression with the collected experimental measurements from the one hundred Douglas-fir and spruce samples described in Chapter 5 gives a coefficient of determination of 79%, and standard error of 0.035. The corresponding regression parameters are $b_1 = 0.145$, and $b_2 = 0.095$.

Figure 6-4 and 6-7 shows that $\overline{P}$ still changes noticeably with grain angle, but $\overline{A}$ does not. To reduce the grain angle effect in the predicted results, model (6-9) is modified to

$$SG = b_1\overline{A} + b_2\overline{P} - b_3\,\overline{A}/\overline{P} \tag{6-10}$$

The third term $\overline{A}/\overline{P}$ in equation (6-10) is added to compensate for some of the grain angle effect induced by $\overline{P}$, because $1/\overline{P}$ and $\overline{P}$ have opposite trends. This term should also reduce the weight of $\overline{A}$ in the evaluation, because *SG* more heavily depends on the phase measurements, as shown in Figure 6-3.

The regression on model equation (6-10) with the same measurements gives a much improved coefficient of determination of 88%, and an improved standard error of 0.026. The resulting calibration parameters are $b_1 = 0.737$, $b_2 = 0.073$, and $b_3 = 1.607$. The equation for determining the specific gravity is then

$$SG = 0.737\overline{A} + 0.073\overline{P} - 1.607\,\overline{A}/\overline{P} \tag{6-11}$$

The results of applying equation (6-11) to the original data from the hundred samples are shown in Figure 6-8 and 6-9. Figure 6-8 shows the estimated *SG* versus the measured *SG* (by oven-dry method). The standard error for the estimated specific gravity is 0.026. For lumber strength grading purposes, this accuracy is satisfactory.

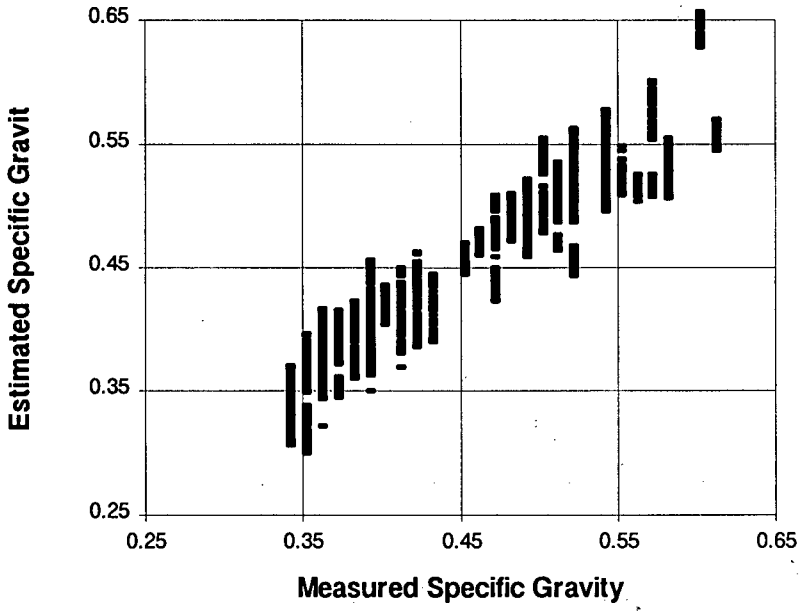

Fig. 6-8 Specific Gravity Determined from Equation (6-11) Using Microwave Measurements vs. Gravimetrically Measured Specific Gravity

Figure 6-9 shows the variation in *SG* determined from the microwave measurements versus the grain angle. The deviation from flatness is primarily carried over from the grain angle dependency of the microwave measurements as shown in Figure 6-1 and 6-5. Figure 6-9 shows the estimated specific gravity of four samples with

different specific gravity versus grain angle. It is seen that the error in the prediction due to the grain angle variation is mostly within the standard error of 0.026. This error is in the range of the overall prediction accuracy, and hence can be considered reasonable.

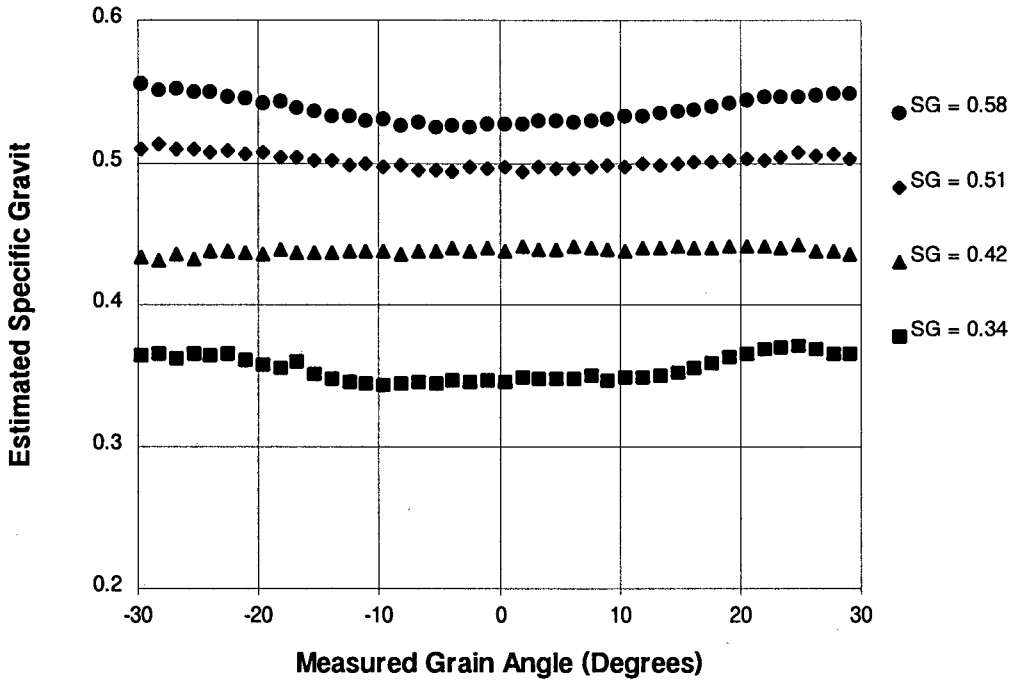

Fig. 6-9 Estimated Specific Gravity vs. Grain Angle

6.5 Moisture Content Determination

Moisture content can be evaluated using Equation (6-7), which is rearranged here as

$$MC = \frac{c_1\overline{A} + c_2\overline{P}}{\overline{A} + c_3\overline{P}}\% \tag{6-12}$$

where c_1, c_2, and c_3 are the corresponding combinations of the coefficients a_1, a_2, a_3, and a_4 in equation (6-7). A nonlinear regression using the microwave measurements on the one hundred measurements described in Chapter 5 gives only a moderate result. The coefficient of determination is 58% with a standard error of 1.2% in *MC*. The resulting equation for determining moisture content is

$$MC = \frac{6.44\overline{A} + 0.83\overline{P}}{\overline{A} + 0.025\overline{P}}\% \tag{6-13}$$

The poor performance of this equation derives from the variations in the microwave measurements due to the grain angle.

In equation (6-13), the two terms in the denominator have very different values. From the experimental data, $\overline{A}$ is generally much larger than $0.025\overline{P}$, except in extreme cases with very high moisture content. Equation (6-12) can be approximated according to the following procedure,

$$
\begin{aligned}
MC &= \frac{c_1\overline{A}+c_2\overline{P}}{\overline{A}+c_3\overline{P}}\% \\
&= \frac{c_1\overline{A}+c_2\overline{P}}{\overline{A}\left(1+c_3\overline{P}/\overline{A}\right)}\% \\
&\approx \frac{c_1\overline{A}+c_2\overline{P}}{\overline{A}}\left(1-c_3\frac{\overline{P}}{\overline{A}}\right)\% \text{ (using the Binomial theorem)} \\
&= \left[c_1+(c_2-c_1c_3)\frac{\overline{P}}{\overline{A}}-c_2c_3\left(\frac{\overline{P}}{\overline{A}}\right)^2\right]\%
\end{aligned}
\tag{6-14}
$$

or

$$
MC = \left[d_1+d_2\frac{\overline{P}}{\overline{A}}+d_3\left(\frac{\overline{P}}{\overline{A}}\right)^2\right]\% \tag{6-15}
$$

where d_1, d_2, and d_3 are the combined coefficients representing the corresponding terms in equation (6-14).

Since equation (6-15) derives from equation (6-12), the moisture content evaluation accuracy of the two equations are similar. A simple linear regression for model (6-15) using the same microwave measurements from the one hundred samples yielded a coefficient of determination of 58% with a standard error of 1.2% in *MC*. The regression parameters are $d_1 = 6.61$, $d_2 = 0.61$, and $d_3 = -0.01$.

It was found that the second-order term in equation (6-15) is not significant. Removing the second-order term in equation (6-15) gives an even simpler model,

$$
MC = \left(d_1+d_2\frac{\overline{P}}{\overline{A}}\right)\% \tag{6-16}
$$

The linear regression of model (6-16) over the same data set gave a coefficient of determination $r^2 = 57\%$, and a standard error of 1.2% in MC with $d_1 = 7.61$ and $d_2 = 0.39$.

The simplicity of model (6-16) is desirable. With a coefficient of determination of 57%, model (6-16) has room for improvement. Considering the fact that the moisture content much more greatly influences the amplitude than the phase change, the performance of model (6-16) may be improved by increasing the weight of the amplitude measurement. Because moisture content and amplitude measurement are inversely related, the term $1/\overline{A}$ is added to the right-hand side of equation (6-16) to increase the presence of the amplitude measurement in the evaluation of moisture content. Therefore, model (6-16) is revised to,

$$MC = \left(d_1 + d_2 \frac{\overline{P}}{\overline{A}} + d_3 \frac{1}{\overline{A}} \right)\% \tag{6-17}$$

A simple linear regression using the same microwave measurements mentioned before gave a coefficient of determination of 85% and a standard error of 0.7% in MC. The resulting equation for determining moisture content from model (6-17) is

$$MC = 2.12 - 0.46 \frac{\overline{P}}{\overline{A}} + 5.95 \frac{1}{\overline{A}} \quad (\%) \tag{6-18}$$

Again, the evaluation equation (6-18) is applied to the original measurement data, the results are shown in Figure 6-10 and 6-11.

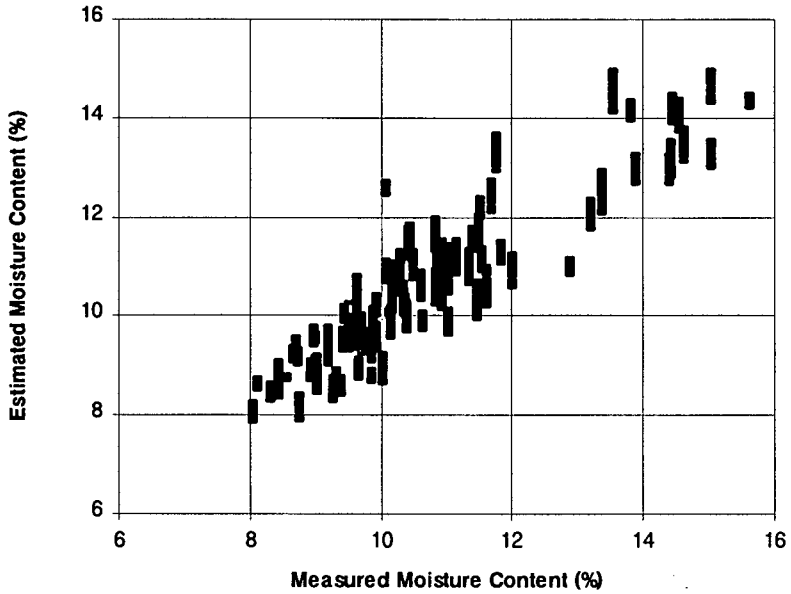

Fig. 6-10 Moisture Content Determined from Equation (6-18) Using Microwave Measurements vs. Gravimetrically Measured Moisture Content

Figure 6-10 shows the *MC* determined using equation (6-18) versus the measured *MC* using oven-dry method. The graph shows the same set of one hundred Douglas-fir and spruce samples described in Chapter 5. The standard error in the estimated moisture content is 0.7% in *MC*. This is certainly sufficient for strength grading purposes.

Figure 6-11 shows the grain angle effect on the evaluated moisture content for four samples with different moisture contents. For grain angles within 30 degrees, Figure 6-11 shows that the variation in the evaluated *MC* is generally within 0.5%. This variation is less than the evaluation error.

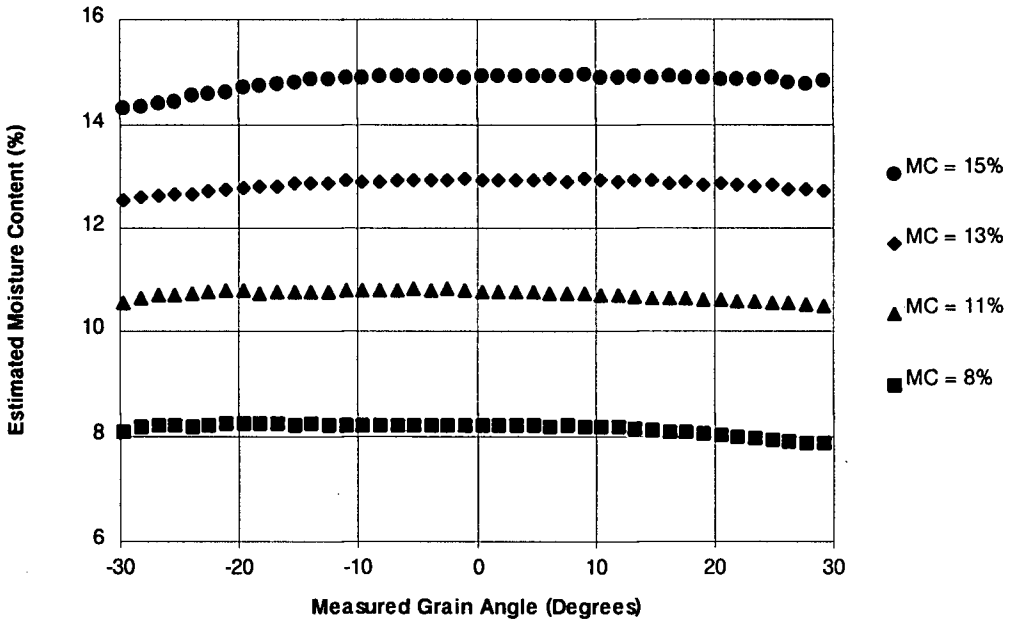

Fig. 6-11 Estimated Moisture Content vs. Grain Angle

The dependence of phase on moisture content is not as strong as the dependence on specific gravity. The grain angle effect in the phase measurement does not significantly influence the results of the estimated moisture content. Because of the weakness of the dependence on grain angle, the raw phase measurement P_0 can be substituted in place of $\overline{P}$ in the evaluation models without serious loss of accuracy. In cases where only moisture content is of interest, the direct phase measurement P_0 should

be used to avoid the need to identify grain angle explicitly. In that case, the amplitude measurement A_{90} is unnecessary.

6.6 Chapter Conclusion

This chapter discussed the use of microwave measurements to determine the specific gravity and moisture content of wood. Using the average of the amplitude measurements from the parallel and the two 45 degree dipoles and the phase change measured from the parallel dipole as indicators, the specific gravity and moisture content are successfully modeled. Using the selected models, the coefficients of determination for specific gravity and moisture content prediction are as high as 88% and 85%, respectively. For the specific gravity, the standard error for evaluation is only 0.026. For the moisture content, the standard error for evaluation is only at 0.7% in *MC*. These results are suitable for strength grading purposes. The required measurements and calculations are straightforward, and are well-suited to real-time grading and quality control applications.

7.0 TEMPERATURE EFFECTS IN THE DETERMINATION OF WOOD PROPERTIES USING MICROWAVE MEASUREMENTS

7.1 Chapter Overview

The dielectric constant of wood is controlled by many molecular characteristics, such as agitation between atoms and polarization of the polar molecules [13]. Temperature change directly influences these molecular activities. All the changes are reflected in the dielectric constants of wood. Therefore, the microwave measurements described in this thesis are expected to be temperature sensitive. This feature is certainly undesirable for microwave equipment to work in sawmills where the environmental temperature changes seasonally. This chapter studies the effects of temperature changes on the microwave amplitude and phase measurements described in the previous chapters. Methods for incorporating temperature effects into the models used for identifying grain angle, specific gravity, and moisture content are then discussed.

7.2 Experimental Observations

All the samples used in chapter 5 and 6 were refrigerated and re-tested using the lab microwave instrumentation system. Each sample was tested at temperatures around

$1^\circ - 6^\circ C$ and $11^\circ - 15^\circ C$. In general, these tests duplicated the measurements described in Chapters 5 and 6, which were conducted during the summer at room temperature of 24°C. Microwave data were collected to examine the effects of temperature.

Figure 7-1 shows example microwave measurements from a Douglas-fir sample with different temperatures, namely $24^\circ C$, $13^\circ C$, and $5^\circ C$. The specific gravity and moisture content of the sample are 0.51 and 10%, respectively.

Figure 7-1 shows that the measurement A_{90} is not sensitive to temperature (the three curves are almost coincident). This is because the dielectric constant in the cross grain direction, α_T, does not significantly vary with temperature at the low moisture contents [28] that are of interest here. This is a desirable feature because A_{90} is the main indicator for grain angle, which is the most important factor responsible for lumber strength.

Figure 7-1 also shows that the measurements A_0 and P_0 all significantly change with temperature. The amplitude measurements decrease with temperature, while the phase measurements increase with temperature. A good feature is that the temperature effects on these measurements are fairly linear and independent of grain angle. The same feature can be extended to the other measurements which are omitted from Figure 7-1 for clarity.

(a)

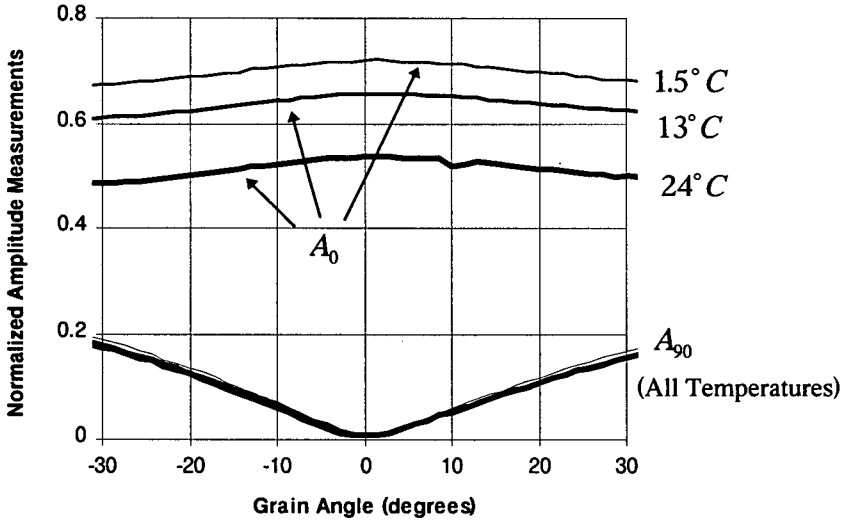

(b)

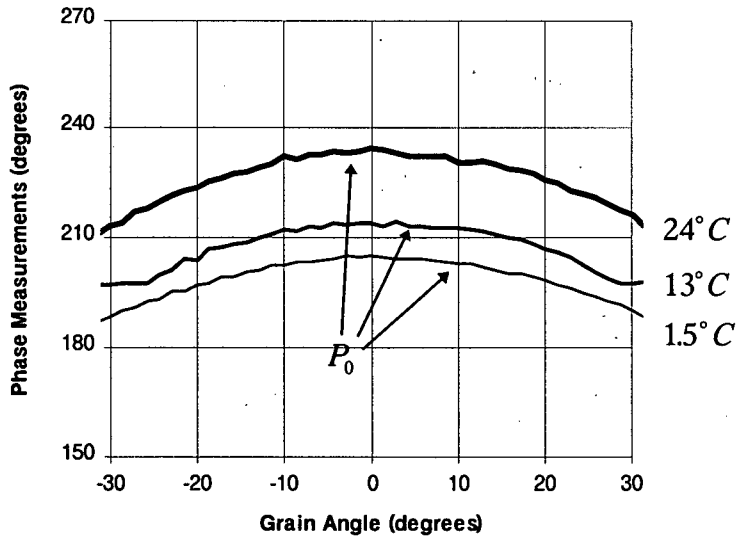

Fig. 7-1 Microwave Measurements vs. Temperature
Douglas-fir Sample: $SG = 0.51$, $MC = 10\%$
(a) Amplitudes A_0 and A_{90} (b) Phase P_0

To illustrate the relationship between the temperature effects and moisture content, Figure 7-2 shows the microwave measurements from another Douglas-fir sample with the same specific gravity, but different moisture content, 16%. Figure 7-2 shows the same general features as Figure 7-1. The two sets of curves indicate that the effect of temperature change increases at higher moisture content.

Figure 7-3 further illustrates the relationship between the temperature effects and specific gravity. It shows the microwave measurements from a Douglas-fir sample with 10% moisture content but different specific gravity, 0.42. Again, Figure 7-3 shows the same general features as the previous two figures. A comparison of the curves indicates that the effect of the temperature change also increases at higher specific gravity, but at a lesser extent than with higher moisture content.

(a)

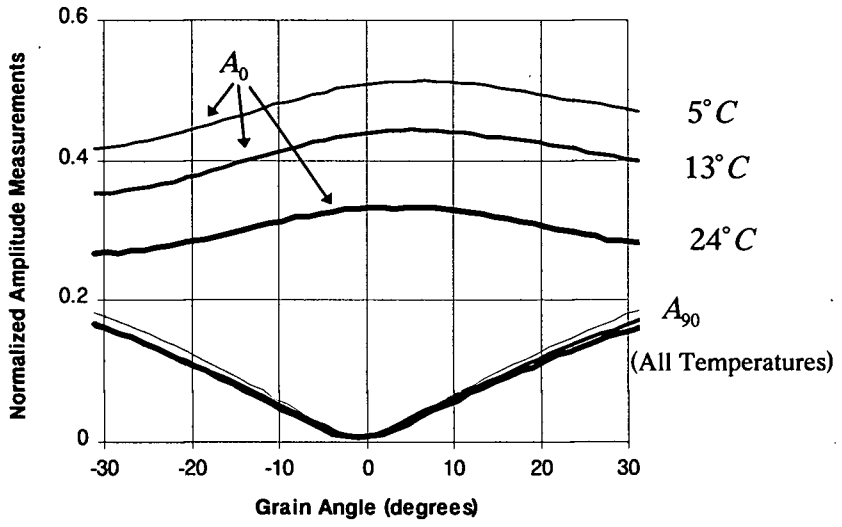

(b)

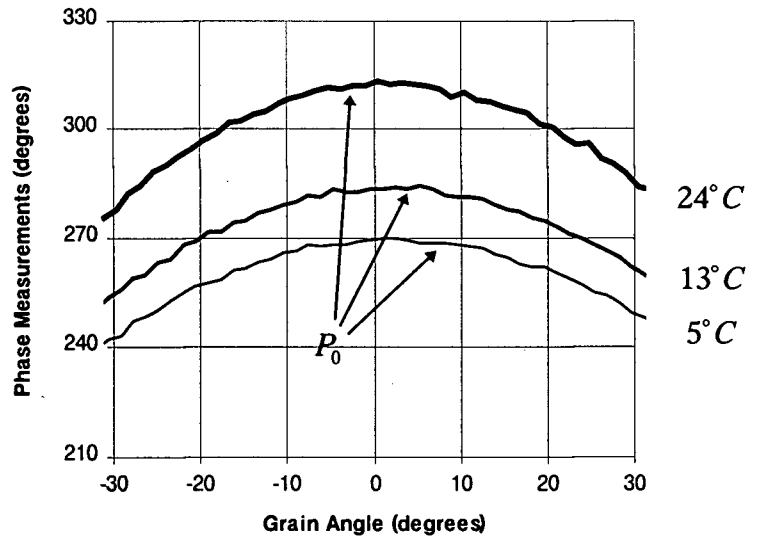

Fig. 7-2 Microwave Measurements vs. Temperature
Douglas-fir Sample: SG=0.51, $MC = 16\%$
(a) Amplitudes A_0 and A_{90} (b) Phase P_0

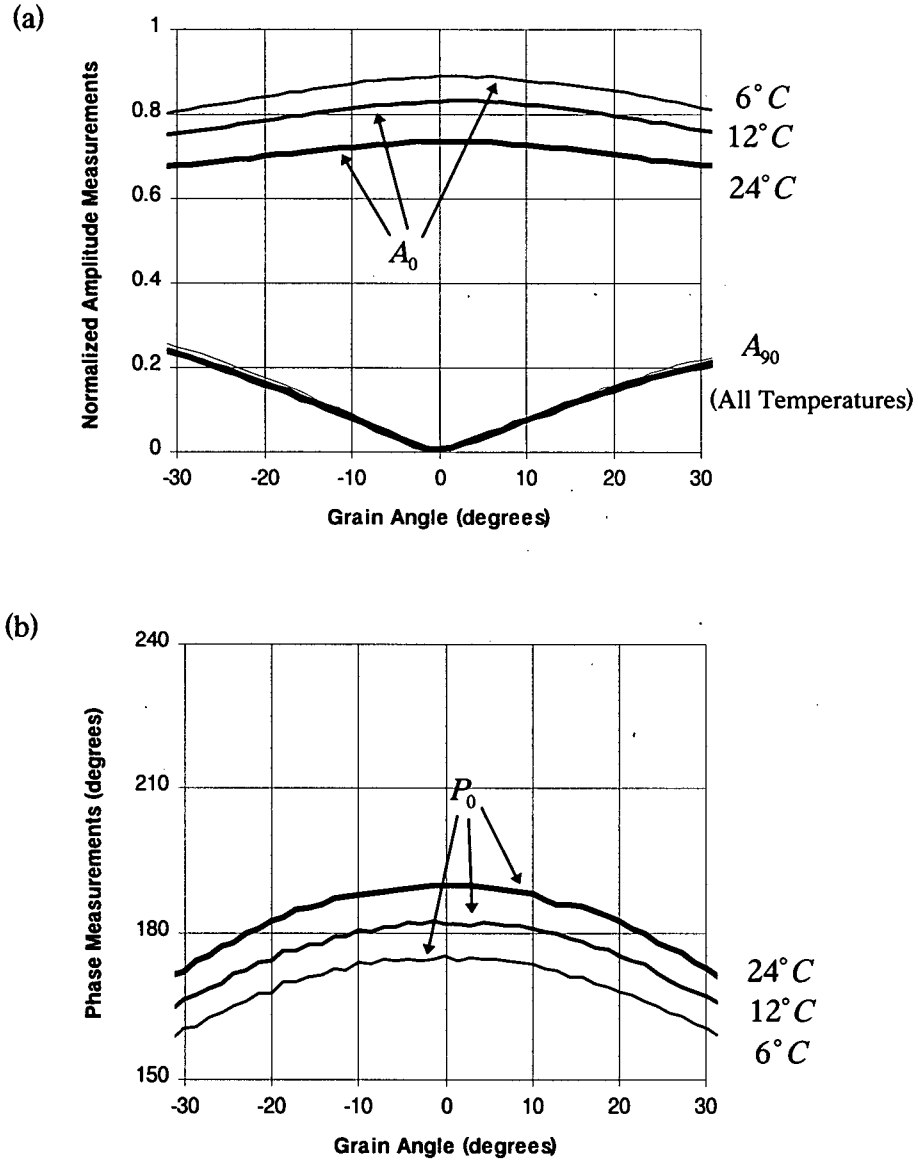

Fig. 7-3 Microwave Measurements vs. Temperature
Douglas-fir Sample: $SG = 0.42$, $MC = 10\%$
(a) Amplitudes A_0 and A_{90} (b) Phase P_0

7.3 Grain Angle Determination with Different Temperatures

In chapter 5, grain angle identification was considered for the constant temperature case. The simplest grain angle evaluation model was equation (5-8), has reproduced as equation (7-1),

$$\hat{\theta} = a_1 (A_{90})^n \tag{7-1}$$

Figures 7-1 to 7-3 indicate that microwave amplitude A_{90} does not vary significantly with temperature change. Therefore, grain angle evaluations using equation (7-1) should be insensitive to temperature changes. This feature was tested by performing a non-linear regression on a data set consisting of the room temperature data from Chapter 5 combined with the low temperature data reported in this chapter. The results are:

$$a_1 = 120, \quad n = 0.88$$

$$r^2 = 94\%, \quad \text{standard error} = 2.0 \text{ degrees.}$$

The corresponding results originally found from the constant temperature measurements in Chapter 5 are

$$a_1 = 121, \quad n = 0.91$$

$$r^2 = 94\%, \quad \text{standard error} = 2.0 \text{ degrees.}$$

These results confirm the temperature independence of grain angle evaluations using equation (7-1).

The effects of specific gravity and moisture content changes can be taken into account to give a more accurate grain angle evaluation. The proposed evaluation model (5-15) includes the effects of these factors. It is reprinted here for convenient reference,

$$\hat{\theta} = c_0 + c_1\left(A_{90}\frac{A_*}{A_0}\right)^n \tag{7-2}$$

As shown in Figure 7-1 to Figure 7-3, the first amplitude term A_{90} varies very little with temperature changes. Figure 7-4 shows example measurements of the second amplitude term A_*/A_0 for a Douglas-fir sample. The graph shows that this ratio also varies very little with temperature. This desirable result occurs because the individual amplitude measurements have similar temperature dependencies that cancel when forming the ratio. Since both amplitude terms in equation (7-1) are almost insensitive to temperature effects, the grain angle evaluation is similarly temperature insensitive, and needs no temperature compensation.

The additional low-temperature data collected for the temperature sensitivity study provides a larger data base on which to determine the coefficients in equation (7-1). Thus, to gain further confidence, a nonlinear regression was performed again on the data used in Chapter 5 combined with the newly collected data at lower temperatures. The results are:

For $-30^\circ \le \hat{\theta} \le 0^\circ$ $\quad c_0 = 1.8,\ c_1 = -96,\ n = 0.78,$
$r^2 = 96\%,$ and Standard Error = 1.75°

For $0° \le \hat{\theta} \le 30°$ $\quad c_0 = -0.8,\ c_1 = 101,\ n = 0.76,$
$r^2 = 95\%,$ and Standard Error = 1.86°

The corresponding results originally found from the constant temperature measurements in Chapter 5 are

For $-30° \le \hat{\theta} \le 0°$ $\quad c_0 = 1.6,\ c_1 = -89,\ n = 0.73,$
$r^2 = 96\%,$ and Standard Error = 1.69°

For $0° \le \hat{\theta} \le 30°$ $\quad c_0 = -1.1,\ c_1 = 98,\ n = 0.74,$
$r^2 = 95\%,$ and Standard Error = 1.78°

The two sets of results are almost identical. Therefore, equation (7-1) for grain angle identification is shown to be temperature insensitive.

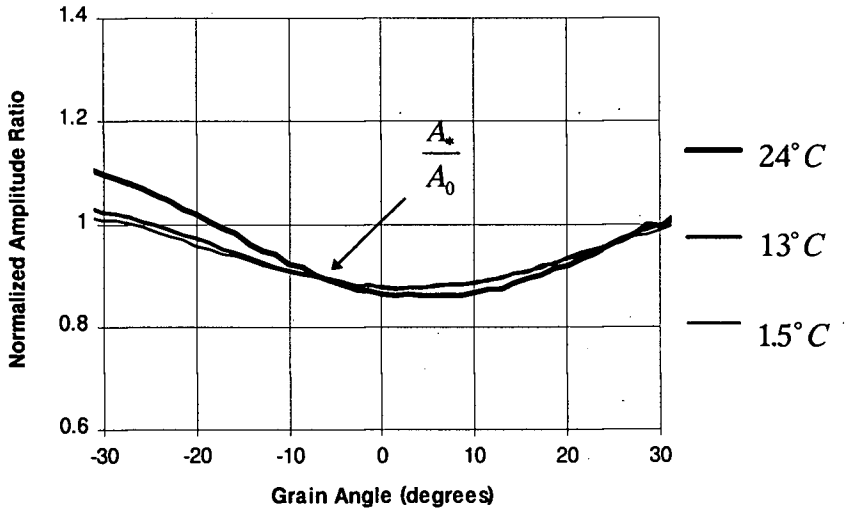

Fig. 7-4 Microwave Amplitude Ratio, A_*/A_0, vs. Temperature
Douglas-fir Sample: $SG = 0.51,\ MC = 10\%$

7.4 Mathematical Expressions of the Temperature Effects in the Amplitude and Phase Measurements.

Figures 7-1 to 7-3 show that the temperature effects on the amplitude and phase measurements are opposite. Higher temperatures cause decrease in amplitude but increase in phase change. This is further illustrated by Figures 7-5 and 7-6. These graphs show that the amplitude measurements change with temperature approximately linearly with the same slope regardless the moisture content and specific gravity. In contrast, the phase measurements show some nonlinearity. The temperature sensitivity of the phase measurements increases at higher specific gravity and also higher moisture content. With these factors in mind, the following simple models of the temperature dependence of the amplitude and phase are proposed,

$$\overline{A}(T) = \overline{A}(T_0) + c_A(T - T_0) \tag{7-3}$$

and

$$\overline{P}(T) = \overline{P}(T_0)\left(1 + c_P(T - T_0)\right) \tag{7-4}$$

where c_A and c_P are the coefficients for the temperature effects in the amplitude and phase measurements, and $T_0 = 24^\circ C$ is the reference temperature.

In keeping with the behavior shown in Figure 7-5 and 7-6, the temperature term in equation (7-3) is independent of amplitude. However, the corresponding term in equation (7-4) is proportional to the phase at the reference temperature, and therefore increases with increase in *SG* and *MC*.

Regression results using the microwave measurements collected at room temperature combined with the low temperature measurements show that equations (7-3) and (7-4) are very effective in describing the temperature effects in the amplitude and phase measurements. For the amplitude measurements using equation (7-3), the results are:

$$c_A = -0.0083 \quad (1/°C), \quad r^2 = 95\%.$$

For the phase measurements using equation (7-4), the results are:

$$c_P = 0.0053 \quad (1/°C), \quad r^2 = 97\%.$$

c_A, and c_P will be used to compensate the effects of temperature change in the determination of the specific gravity and moisture content.

(a)

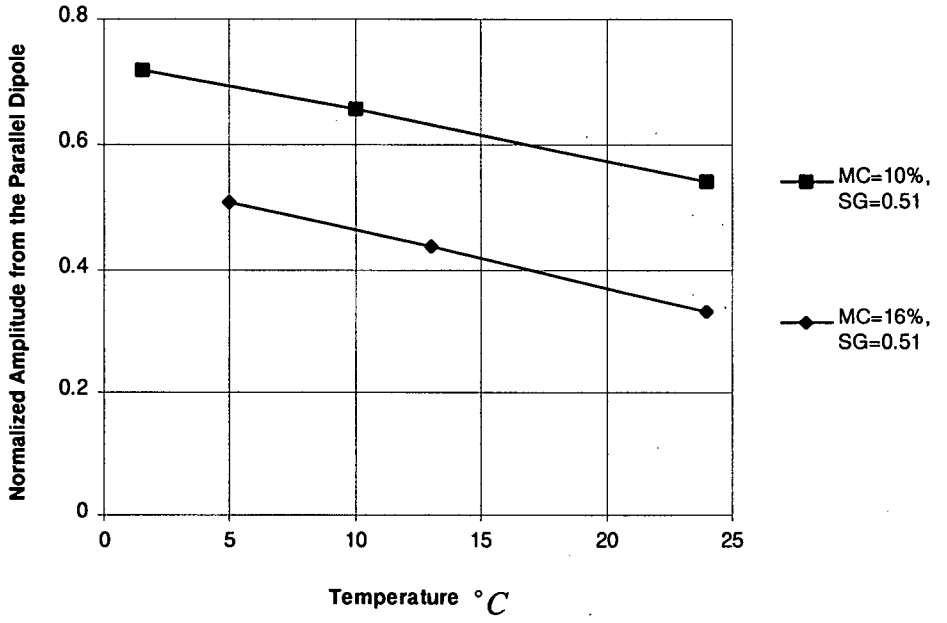

(b)

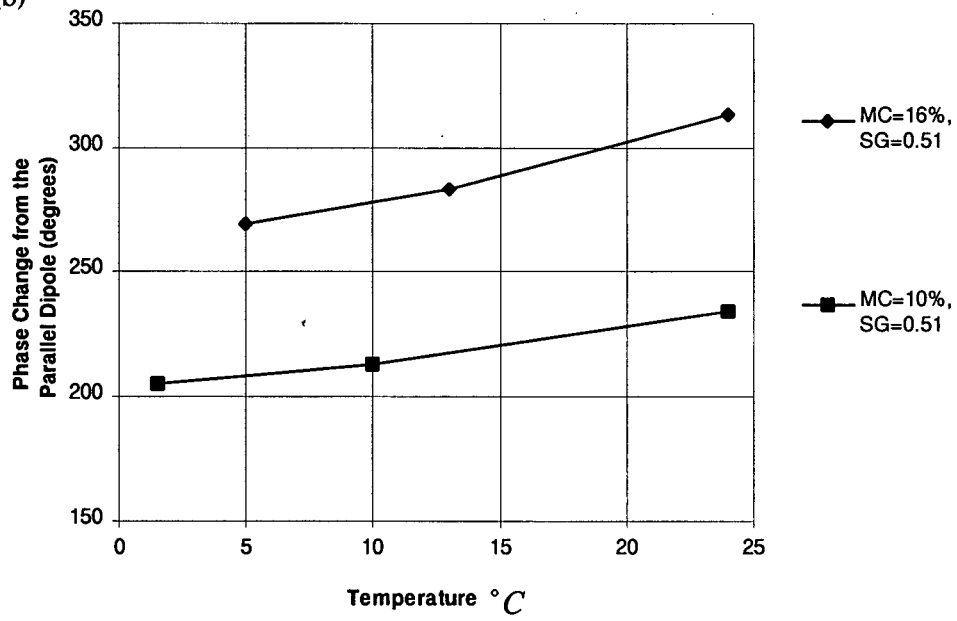

Fig. 7-5 Microwave Measurements at 0° Grain Angle
vs. Temperature with Different Moisture Content
Douglas-fir Sample: $SG = 0.51$, $MC = 10\%$ and 16%
(a) Amplitudes A_0 (b) Phase P_0

(a)

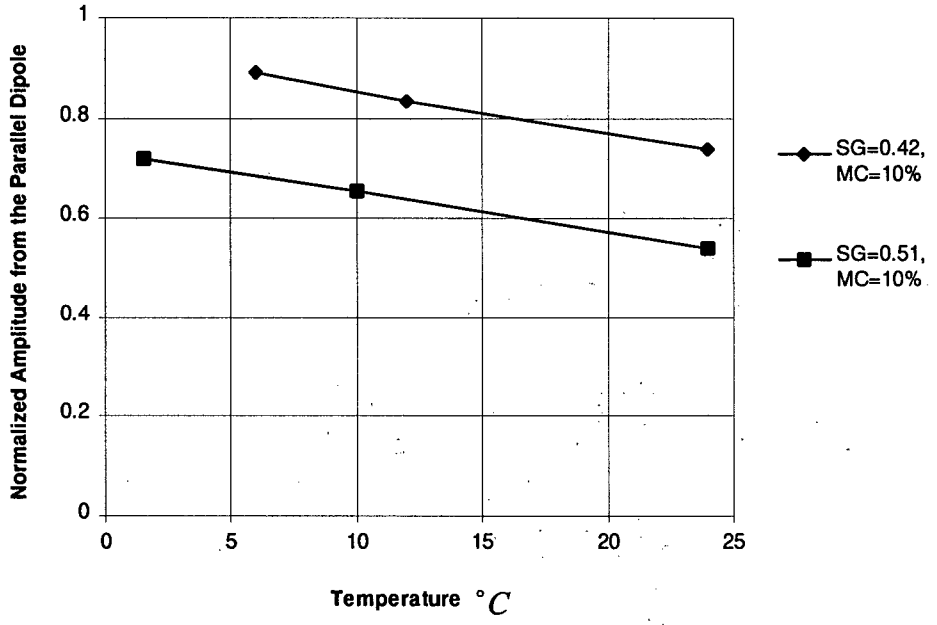

(b)

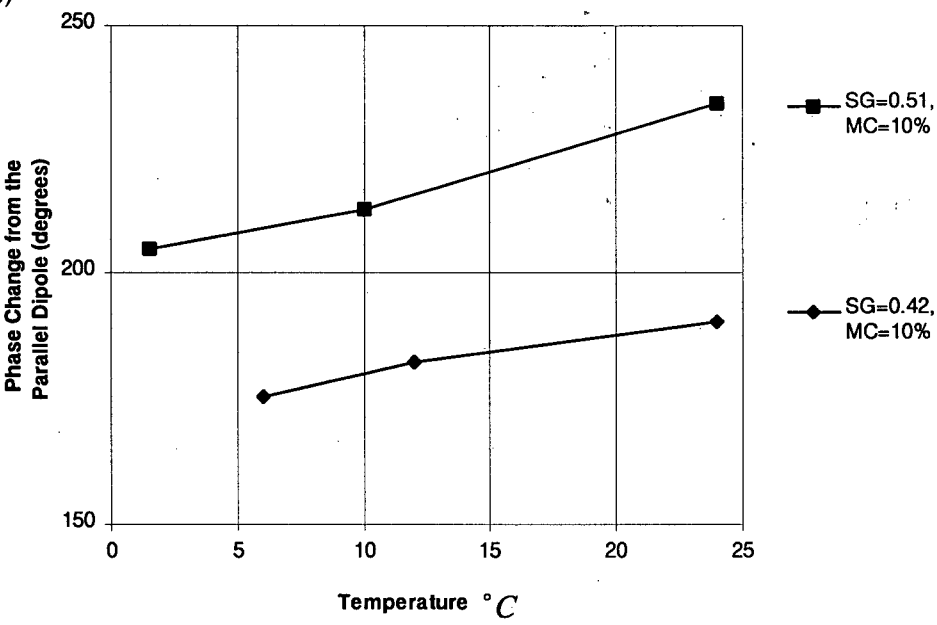

Fig. 7-6 Microwave Measurements at 0° Grain Angle vs. Temperature with Different Specific Gravity Douglas-fir Sample: $SG = 0.42$ and 0.51, $MC = 10\%$
(a) Amplitudes A_0 (b) Phase P_0

7.5 Specific Gravity Determination with Temperature Effects

For convenience, the model equation (6-10) for specific gravity evaluation discussed in Section 6.4 is reproduced here

$$SG = b_1\overline{A}(T_0)+b_2\overline{P}(T_0)-b_3\,\overline{A}(T_0)/\overline{P}(T_0) \tag{7-5}$$

In equation (7-5) the reference temperature is indicated explicitly. Combining Equations (7-3) to (7-5), a new model for specific gravity evaluation with temperature effects can be derived, i.e.,

$$\begin{aligned} SG = {} & b_1\left(\overline{A}-c_A(T-T_0)\right) + b_2\frac{\overline{P}}{\left(1+c_P(T-T_0)\right)} \\ & - b_3\frac{\left(\overline{A}-c_A(T-T_0)\right)\left(1+c_P(T-T_0)\right)}{\overline{P}} \end{aligned} \tag{7-6}$$

From section 7.4, $c_A = -0.0083$ and $c_P = 0.0053$. Equation (7-6) can then be written

$$\begin{aligned} SG = {} & b_1\left(\overline{A}+0.0083(T-T_0)\right) + b_2\frac{\overline{P}}{\left(1+0.0053(T-T_0)\right)} \\ & - b_3\frac{\left(\overline{A}+0.0083(T-T_0)\right)\left(1+0.0053(T-T_0)\right)}{\overline{P}} \end{aligned} \tag{7-7}$$

A nonlinear regression was performed for model (7-7) using the original data set collected at room temperature combined with the low-temperature data. The results are:

$$b_1 = 0.61,\quad b_2 = 0.078,\quad b_3 = 1.30,$$

$$r^2 = 86\%, \text{ and standard error} = 0.028$$

Although it gives good results, the use of equation (7-7) is inconvenient because it requires explicit knowledge of the wood temperature. The question arises as to the consequence of neglecting the temperature effects.

Again, a non-linear regression was performed, this time on model (7-6) with coefficients c_A and c_P both set to zero. This is equivalent to equation (7-5) without the temperature reference. The regression results based on the combined room temperature and low temperature data are:

$$b_1 = 0.580,\ b_2 = 0.077,\ b_3 = 1.138,$$

$$r^2 = 86\%, \text{ and standard error} = 0.029.$$

The corresponding regression results for the room temperature data alone, from Chapter 6 are:

$$b_1 = 0.737,\ b_2 = 0.073,\ b_3 = 1.607,$$

$$r^2 = 88\%, \text{ and standard error} = 0.026.$$

The above results show that no serious accuracy degradation occurs when identifying *SG* without temperature compensation. It turns out that most of the temperature effects in the microwave measurements in model (7-5) cancel out because the temperature effects on amplitude and phase measurements are opposite. The recommended evaluation equation is therefore

$$SG = 0.580\overline{A} + 0.077\overline{P} - 1.138\,\overline{A}/\overline{P} \qquad (7\text{-}7)$$

The work in this section demonstrates that the discussion on the evaluation of specific gravity in Chapter 6 is still valid in a environment of changing temperature. The model equation (6-7) is effective for measurements with different temperatures though the temperature effects on the microwave measurements are significant. Explicit knowledge of temperature is not necessary for determining specific gravity.

7.6 Moisture Content Determination with Temperature Effects

The model equation (6-17) for moisture content evaluation is quoted below as equation (7-8),

$$MC = \left(d_1 + d_2 \frac{\overline{P}(T_0)}{\overline{A}(T_0)} + d_3 \frac{1}{\overline{A}(T_0)} \right)\% \tag{7-8}$$

After substituting equations (7-4) and (7-5) into (7-8) to accommodate temperature effects, the result is

$$MC = \left[d_1 + d_2 \frac{\overline{P}}{\left(1 + c_P (T - T_0)\right)\left(\overline{A} - c_A (T - T_0)\right)} + d_3 \frac{1}{\left(\overline{A} + c_A (T - T_0)\right)} \right]\% \tag{7-9}$$

From section 7.4, $c_A = -0.0083$ and $c_P = 0.0053$. Equation (7-9) can therefore be written as

$$MC = \left[d_1 + d_2 \frac{\overline{P}}{(1 + 0.0053(T - T_0))(\overline{A} + 0.0083(T - T_0))} + d_3 \frac{1}{(\overline{A} + 0.0083(T - T_0))} \right] \% \tag{7-10}$$

A regression was performed for equation (7-10) using the combined room temperature and low temperature data. The results are,

$$d_1 = 2.95, d_2 = -0.30, \; d_3 = 5.21,$$

$$r^2 = 77\%, \text{ and standard error} = 0.9\% \text{ in } MC.$$

Equation (7-10) is useful only in the case where the temperature is known. The required temperature measurement is an undesirable complication. Therefore, the question again arises as to whether the original model (7-9) may still be able to give a reasonable estimation of moisture content without temperature compensation. This question was examined by performing a regression of equation (7-9) using the combination of the room temperature and low temperature data. The results are

$$MC = \left(4.74 - 0.254 \frac{\overline{P}}{\overline{A}} + 4.50 \frac{1}{\overline{A}} \right) \% \tag{7-11}$$

$$r^2 = 54\%, \text{ Standard Error } = 1.2\% \text{ in } MC.$$

Though the evaluation results using model (7-11) are considerably worse than model (7-10) in the case of moisture content evaluation, the accuracy could be sufficient for applications where the accuracy of MC is not strict. Model (7-11) eliminates the need of temperature measurement, and thus is desirable where knowledge of the temperature is

difficult to obtain. If higher moisture content measurement accuracy is needed, then explicit wood temperature measurement has to be made.

7.7 Chapter Conclusion

This chapter discussed the temperature effects in the microwave measurements for determining the grain angle, the specific gravity and moisture content. It is found that the models developed in Chapter 5 and 6 for grain angle and specific gravity evaluation remain effective at different temperatures. A good feature in these models is that temperature effects are contained implicitly, therefore explicit temperature measurement is not required.

Temperature knowledge is needed to obtain accurate moisture content evaluations. However, the required temperature compensation, equation (7-10), is straightforward and adds minimal numerical complication. It is also found that moisture content can be estimated without explicit temperature measurement for applications where less accurate estimates of moisture content are sufficient. In conclusion, the current microwave instrumentation system is effective in providing grain angle, specific gravity, and moisture content in an environment with changing temperature.

8.0 CONCLUSIONS

8.1 Overall Conclusions

The work described in this thesis is the first part of a project for developing an advanced lumber strength grading system using microwave measurements. The overall objective is to develop an improved practical system for estimating lumber strength. This will enable lumber to be graded more accurately, thereby improving its utilization efficiency and economic value, and reducing the need for excessively conservative structural design.

A microwave instrumentation system is described in this thesis that can measure wood grain angle, specific gravity, and moisture content. These three physical properties directly influence lumber strength. Local measurement of these three quantities provide a strong starting point for improved lumber strength estimations.

In the development of the current microwave instrumentation system, an advanced microwave sensor system was designed to measure elliptically polarized microwave fields. The sensor contains four independent scattering dipoles with a common geometric center. This sensor provides four microwave measurements at each measurement point without need for a mechanical rotation mechanism. This feature not only substantially speeds up the measurement process compared to designs requiring mechanical rotation, but also allows more flexible settings, i.e., both reflection and

transmission measurements. Numerical methods based on theoretical analysis are also presented to identify elliptically polarized microwave fields from the microwave amplitude measurements. The experiments showed that the results from the new method are very promising.

The experiments confirmed that the microwave measurements using the new 4-dipole microwave sensor successfully indicate wood properties. The new microwave sensor was developed to measure wood grain angle, specific gravity, and moisture content. A simplified microwave theory was developed to describe the relationship between the measurements from each sensor dipole and wood grain angle, specific gravity, and moisture content. The simplified theory is very successful in explaining the experimental observations, and provides valuable guidance in the modeling of the microwave measurements for predicting grain angle, specific gravity, and moisture content.

The effects of different wood structural and geometric characteristics on the microwave measurements were also studied. It was found that the annual ring direction of wood has very little effect on the microwave measurements. This convenient characteristic occurs because the dielectric properties of wood in the tangential and radial directions are very similar. Experimental observations also indicated that the presence of moderate amounts of diving grain do not affect the microwave measurements significantly. Theoretical analysis and experimental measurements both confirmed that limited variations in lumber thickness do not greatly affect the microwave measurements. All these features in the microwave measurements simplify the modeling of grain angle,

specific gravity, and moisture content, and make it possible to achieve reliable predictions of these wood properties.

Starting from the simplified microwave theory, a simple but efficient model was developed for predicting the grain angle using the microwave measurements from the newly developed microwave sensor. For data collected from a hundred samples of Douglas-fir and spruce, the model gave a coefficient of determination $r^2 = 95\%$, and a standard error of 1.8 degrees for grain angles up to 30 degrees. The estimation error also has a favorable trend, i.e., the error is smaller for smaller grain angles and it is larger for larger grain angles. This feature is desirable because most of the strength reduction in lumber due to grain angle occurs at smaller grain angles. Therefore, accurate grain angle determination is more important for small grain angles than for large angles.

Though the shapes of the microwave amplitude measurements from the multiple-dipole sensor are quite complicated, the models for evaluating specific gravity and moisture content developed in this thesis are quite simple. For specific gravity, the proposed evaluation model gives a coefficient of determination $r^2 = 88\%$, and a standard error of 0.026. For moisture content, the proposed evaluation model gives a coefficient of determination of 85% and a standard error of 0.7% in *MC*.

Because the temperature in a sawmill changes seasonally over a substantial range, the effects of temperature on microwave measurements and on the resulting evaluations of grain angle, specific gravity, and moisture content were studied in detail. The effects of temperature on the microwave measurements was found to be quite significant. To eliminate these unwanted effects, models were developed to evaluate grain angle and

specific gravity that internally compensate for the changes induced by temperature effects. As a result, temperature does not need to be considered explicitly in the evaluation of grain angle and specific gravity. It was also found that temperature measurement is needed only when accurate moisture content results are required. Without the knowledge of temperature, moisture content can still be determined, but with a lesser accuracy. In this case, the standard error rises to 1.2% in *MC*. This larger error is still sufficient for most practical applications. In summary, temperature effects are not critical in the current microwave instrumentation system for accurate prediction of grain angle, specific gravity, and moisture content. This feature is desirable especially in cases where the ambient temperature can vary over a wide range.

The current microwave instrumentation system developed during this thesis research can provide accurate grain angle, specific gravity, and moisture content in real-time regardless of environmental temperature, wood species, and wood structural characteristics such as annual ring direction, diving grain, and small thickness variation. Accurate knowledge of grain angle, specific gravity, and moisture content will make it possible to calculate lumber strength using mechanistic procedures. Since mechanistic calculations model actual wood physical behavior, they are expected to handle effectively the large variations that naturally occur in commercial lumber. In contrast, statistically based methods deteriorate in effectiveness when the graded material deviates in any significant way from the lumber sample used for the original strength correlation testing.

Though the current study is aimed at the development of a new generation of lumber strength grading systems, the instrumentation system and methodology presented

here can also be used in a wide range of applications for property measurement and quality control of wood products and wood production processes.

8.2 Specific Contributions

Besides the framework and procedure for using microwaves to measure localized wood properties, this thesis has made several specific contributions:

1. the 4-dipole microwave sensor design;
2. application of the 4-dipole sensor for measuring elliptically polarized microwave fields;
3. formulation of simplified equations for using the 4-dipole sensor to measure wood properties;
4. identification of uncoupled variables for independently estimating wood grain angle, specific gravity, and moisture content;
5. formulation mathematical models for independently estimating grain angle, specific gravity, and moisture content;
6. formulation of implicit and explicit temperature compensations in the estimation of grain angle, specific gravity, and moisture content.

REFERENCES

1. Wood Handbook: Wood as An Engineering Material. Agriculture Handbook 72, Forest Products Laboratory, Forest Services, U.S. Department of Agriculture, 1987.

2. Galligan, W. L.; Green, D. W. Development of Standardized Concepts for Assignment and Assessment of the Mechanical Properties of Lumber. Forest Products Journal, 30(9), 1980.

3. Hilbrand, H. C.; Miller, D. G. Machine Grading - Theory and Practice. Forest Products Journal, 16(11), 1966.

4. Barrett, J. D.; Lau, W. Bending strength adjustments for moisture content for structural lumber. Wood Science and Technology, 25, pp. 433-447, 1991.

5. Barrett, J. D.; Lau, W. Compression strength adjustments for moisture content in Douglas-Fir structural lumber. Wood and Fiber Science, 23(4), pp. 543-557, 1991.

6. Cramer, S. M.; McDonald, K. A. Predicting lumber tensile stiffness and strength with local grain angle measurements and failure analysis. Wood and Fiber Science, 21(4), pp. 393-410, 1989.

7. Cramer, S. M.; Goodman, J. R. Failure modeling: a basis for strength prediction of lumber. Wood and Fiber Science, 18(3), pp. 446-459, 1986.

8. Bechtel, F. K.; Allen, J. R. Methods of implementing grain angle measurements in the machine stress rating process. Proceedings of the 6th Non-destructive Testing Wood Symposium, Pullmann, Washington, 1987.

9. Bechtel, F. K.; Allen, J. R. Non-destructive testing methods for lumber. U.S. Patent Number 4,926,350, May 15, 1990.

10. Samson, M.; Blanchet, L. Effect of knots on the flatwise bending stiffness of lumber members. Holz, 50, pp. 148-152, 1992.

11. Schajer, G. S. Method for estimating the strength of wood. U.S. Patent Number 4,941,357, July 17, 1990.

12. Clauson, M. L.; Wilson, J. B. Comparison of video and x-ray for scanning wood density. Forest Products Journal, 41(3), 1991.

13. Yavorsky, J. M. A review of electrical properties of wood. Technical Publication No. 73, College of Forestry, State University of New York at Syracuse, 1951.

14. Peyskens, E.; Pourcq; Stevens, M.; Schalck, J. Dielectric properties of softwood species at microwave frequencies. Wood Science and Technology, 18, pp. 267-280, 1984.

15. James, W. L.; Hamill, D. Dielectric properties of Douglas-fir measured at microwave frequencies. Forest Products Journal, 15, pp. 51-56, 1965.

16. King, R. J. Microwave sensors for process control, Part I and II. Sensors, October 1992, pp. 25-29.

17. Kraszewski, A. W. Microwave aquametry - Needs and Perspectives. IEEE Transactions on Microwave Theory and Techniques, 39(5), 1991.

18. Kraszewski, A. W. Microwave aquametry - A Review. Journal of Microwave Power, 15(4), 1980.

19. King, R. J.; Basuel, J. C. Measurement of basis weight and moisture content of composite boards using microwaves. Forest Products Journal, 43(9), 1993.

20. King, R. J.; King, K. V.; Woo, K. Microwave moisture measurement of grains. IEEE Transactions on instrumentation and measurement, 41(1), 1992.

21. Kraszewski, A. Microwave monitoring of moisture content in grain. Journal of Microwave Power and Electromagnetic Energy, 23(4), 1988.

22. Bramanti, M. A slot line microwave dielectric permittivity sensor for measure and control of laminated materials. Journal of Microwave Power and Electromagnetic Energy, 26(2), 1991.

23. Cutmore, N.; Evans, T.; McEwan, A. On-Conveyor determination of moisture in coal. Journal of Microwave Power and Electromagnetic Energy, 26(4), 1991.

24. Audet, A.; Bolomey, J. C.; et al. Electrical characteristics of waveguide applicators for medical applications. Journal of Microwave Power, 15(3), 1980.

25. R. J. King. Microwave Homodyne Systems. IEE Electromagnetic Wave Series 3, Peter Pergrinus, Ltd., Stevenage, England, 1978.

26. McLauchlan, T. A.; Norton, J. A.; Kusec, D. J. Slope-of-Grain Indicator. Forest Products Journal, 23(5), 1973.

27. Steele, P. H.; Neal, S. C.; McDonald, K. A.; Cramer, S. M. The slope-of-grain indicator for defect detection in unplaned hardwood lumber. Forest Products Journal, 41(1), 1991.

28. Yen, Y. H. Microwave electromagnetic nondestructive testing of wood in real time. Ph.D. dissertation, Department of Electronic and Computer Engineering, University of Wisconsin, 1981.

29. King, R. J. On airborne wave tilt measurements. Radio Science, 12(3), pp. 405-414, 1977.

30. King, R. J.; Yen, Y. H. Probing amplitude, phase, and polarization of microwave field distributions in real time. IEEE Transactions on Microwave Theory and Techniques, 29(11), 1981.

31. King, R. J. Microwave Electromagnetic Nondestructive Testing of Wood. Proceedings of the 4th Nondestructive Testing of Wood Symposium, Vancouver, Washington, 1978.

32. Shen, J.; Schajer, G.; Parker, R. A new probe for characterizing elliptically polarized microwave fields. Journal of Microwave Power and Electromagnetic Energy, 28(4), 1993.

33. Madsen, B. Strength values for wood and limit states design. Canadian Journal of Civil Engineering, 2(3), pp. 270-279, 1975.

34. Madsen, B. In-grade testing --- problem analysis. Forest Products Journal, 28(4), pp. 42-50, 1978.

35. Johnson, R.A. Current statistical methods for estimating lumber properties by proofloading. Forest Products Journal, 30(1), pp. 14-22, 1980.

36. Bechtel, F.K. Proof test load value determination for maximum economic return. Forest Products Journal, 33(10), pp. 30-38, 1983.

37. Madsen, B. STRUCTURAL BEHAVIOR OF TIMBER. Timber Engineering Ltd., 1992.

38. PRECISION TESTING EQUIPMENT FOR WOOD. Catalog 21-1, Metriguard Inc., Pullman, Washington, U.S.A.

39. Gerhards, C.C. Longitudinal stress waves for lumber stress grading: factors affecting applications: state of the art. Forest Products Journal, 32(2), pp. 20-25, 1982.

40. DeBonis, A.L. Stress waves produce lumber strength data. Forest Industries, pp. 32-33, March 1986.

41. Sandoz, J.L. Grading of construction timber by ultrasound. Wood Science and Technology, 23, pp. 95-108, 1989.

42. Bender, D.A.; Burk, A.G.; Taylor, S.E.; Hooper, J.A. Predicting localized tensile strength in solid and finger-jointed laminating lumber using longitudinal stress waves. Forest Products Journal, 40(3), pp. 45-47, 1990.

43. Corder, S.E. Localized deflection related to bending strength of lumber. Proc. Second Symposium on Nondestructive Testing of Wood, Spokane, Washington, U.S.A., 1965.

44. Endersby, H.J. Survey of machine stress grading. Proc. IUFRO Meeting, Working Group on Structural Utilization, Vol. II, pp. 149-176, Forest Products Research Lab., Princes Risborough, England, 1969.

45. Samson, M.; Hailey, R.T. Status of machine stress-rating of lumber 25 years after commercial implementation. Forest Products Journal, 39(11), pp. 49-52, 1989.

46. G.I., Torgovnikov. DIELECTRIC PROPERTIES OF WOOD AND WOOD-BASED MATERIALS. Springer Series in Wood Science, 1993.